Mutations in the Chromatin Regulator Gene *BRPF1* Cause Syndromic Intellectual Disability and Deficient Histone Acetylation

Kezhi Yan,[1,17] Justine Rousseau,[2,17] Rebecca Okashah Littlejohn,[3] Courtney Kiss,[4] Anna Lehman,[5] Jill A. Rosenfeld,[6] Constance T.R. Stumpel,[7] Alexander P.A. Stegmann,[7] Laurie Robak,[6] Fernando Scaglia,[6] Thi Tuyet Mai Nguyen,[2] He Fu,[2] Norbert F. Ajeawung,[2] Maria Vittoria Camurri,[2] Lin Li,[1] Alice Gardham,[8] Bianca Panis,[9] Mohammed Almannai,[6] Maria J. Guillen Sacoto,[10] Berivan Baskin,[10] Claudia Ruivenkamp,[11] Fan Xia,[6] Weimin Bi,[6] DDD Study,[12] CAUSES Study,[5] Megan T. Cho,[10] Thomas P. Potjer,[11] Gijs W.E. Santen,[11] Michael J. Parker,[13] Natalie Canham,[8] Margaret McKinnon,[5] Lorraine Potocki,[6] Jennifer J. MacKenzie,[4,14] Elizabeth R. Roeder,[3,6] Philippe M. Campeau,[2,15,*] and Xiang-Jiao Yang[1,16,*]

Identification of over 500 epigenetic regulators in humans raises an interesting question regarding how chromatin dysregulation contributes to different diseases. Bromodomain and PHD finger-containing protein 1 (BRPF1) is a multivalent chromatin regulator possessing three histone-binding domains, one non-specific DNA-binding module, and several motifs for interacting with and activating three lysine acetyltransferases. Genetic analyses of fish *brpf1* and mouse *Brpf1* have uncovered an important role in skeletal, hematopoietic, and brain development, but it remains unclear how BRPF1 is linked to human development and disease. Here, we describe an intellectual disability disorder in ten individuals with inherited or de novo monoallelic *BRPF1* mutations. Symptoms include infantile hypotonia, global developmental delay, intellectual disability, expressive language impairment, and facial dysmorphisms. Central nervous system and spinal abnormalities are also seen in some individuals. These clinical features overlap with but are not identical to those reported for persons with *KAT6A* or *KAT6B* mutations, suggesting that BRPF1 targets these two acetyltransferases and additional partners in humans. Functional assays showed that the resulting *BRPF1* variants are pathogenic and impair acetylation of histone H3 at lysine 23, an abundant but poorly characterized epigenetic mark. We also found a similar deficiency in different lines of *Brpf1*-knockout mice. These data indicate that aberrations in the chromatin regulator gene *BRPF1* cause histone H3 acetylation deficiency and a previously unrecognized intellectual disability syndrome.

Introduction

Epigenetic regulation is essential for human development and becomes aberrant in different diseases. The human genome encodes over 500 epigenetic regulators.[1–3] To date, ~30 chromatin modifiers have been associated with human diseases, including the ATP-dependent helicases CHD4, CHD7, CHD8, SMARCA2, SMARCA4, and ATRX;[4–6] the DNA methyltransferases DNMT1 and DNMT3b;[4] the histone methyltransferases EZH2 and KMT3B;[4] the lysine acetyltransferases CREBBP, EP300, KAT6A, KAT6B, and ESCO2;[4,7–14] and the histone deacetylases HDAC4 and HDAC8.[15,16] By contrast, disease association remains much less clear for hundreds of chromatin readers that utilize structural modules to sense DNA and histone modification states for chromatin-based signaling.[17,18] Thus, it is important to identify disease links for such chromatin readers. Bromodomain and PHD finger-containing protein 1 (BRPF1) is a multivalent chromatin reader composed of multiple nucleosome-binding modules, including double PHD fingers (linked with a C2HC zinc knuckle), a bromodomain, and a PWWP domain.[19–21] The PHD fingers and zinc knuckle form a bivalent nucleosome-binding unit, known as the PZP (PHD finger–zinc knuckle–PHD finger) domain.[22,23] In addition, BRPF1 possesses two enhancer of polycomb (EPC)-like motifs flanking the PZP domain.[19–21] Through one of these EPC-like motifs and its N-terminal region, BRPF1 interacts with and activates three histone acetyltransferases, KAT6A, KAT6B, and KAT7.[19–21] Thus, BRPF1 is a unique chromatin reader that also possesses

[1]Rosalind & Morris Goodman Cancer Research Center and Department of Medicine, McGill University, Montreal, QC H3A 1A3, Canada; [2]CHUSJ Research Center, CHU Sainte-Justine, Montreal, QC H3T 1J4, Canada; [3]Department of Pediatrics, Baylor College of Medicine, San Antonio, TX 77030, USA; [4]Kingston General Hospital, 76 Stuart Street, Armstrong 4, Kingston, ON K7L 2V7, Canada; [5]Department of Medical Genetics, University of British Columbia, 4500 Oak Street, Vancouver, BC V6H 3N1, Canada; [6]Department of Molecular and Human Genetics, Baylor College of Medicine, One Baylor Plaza, Houston, TX 77030, USA; [7]Department of Clinical Genetics and School for Oncology & Developmental Biology, Maastricht University Medical Center, Maastricht 6229, the Netherlands; [8]North West Thames Regional Genetics Service, London North West Healthcare NHS Trust, Northwick Park Hospital, Watford Road, Harrow HA1 3UJ, UK; [9]Department of Pediatrics, Zuyderland Medical Center, Heerlen and Sittard 6419, the Netherlands; [10]GeneDx, 207 Perry Parkway, Gaithersburg, MD 20877, USA; [11]Department of Clinical Genetics, Leiden University Medical Center, Leiden 2300RC, the Netherlands; [12]Decipher Developmental Disorder Study, Wellcome Trust Sanger Institute, Wellcome Genome Campus, Hinxton CB10 1SA, UK; [13]Sheffield Clinical Genetics Service, OPD2, Northern General Hospital, Herries Road, Sheffield S5 7AU, UK; [14]Division of Clinical Genetics, Department of Pediatrics, McMaster University, Hamilton, ON L8S 4K1, Canada; [15]Department of Pediatrics, Sainte-Justine Hospital and University of Montreal, QC H3T 1J4, Canada; [16]Department of Biochemistry, McGill University and McGill University Health Center, Montreal, QC H3A 1A3, Canada
[17]Co-first authors
*Correspondence: p.campeau@umontreal.ca (P.M.C.), xiang-jiao.yang@mcgill.ca (X.-J.Y.)
http://dx.doi.org/10.1016/j.ajhg.2016.11.011.

sequence motifs mediating interaction with histone acetyltransferases.

Zebrafish and mouse genetic studies have shown that *Brpf1* is essential for embryo survival, hematopoiesis, head patterning, and brain development.[24–29] Moreover, mutations in *KAT6A* (MIM: 601408) and *KAT6B* (MIM: 605880) have recently been discovered in multiple individuals with several developmental disorders characterized by intellectual disability and other abnormalities.[7–13] Thus, an interesting question is whether mutations of human *BRPF1* (MIM: 602410) cause similar developmental anomalies. Here, we report that heterozygous missense, nonsense, and reading frameshift mutations in this gene cause a neurodevelopmental disorder characterized by congenital hypotonia, global developmental delay, intellectual disability, and facial dysmorphisms. We show that these mutations cause deficiency of histone H3K23 acetylation and provide evidence that BRPF1 acts through KAT6A and KAT6B to govern this chromatin modification in vitro and in vivo. Together, this study and the recent reports on individuals with *KAT6A* and *KAT6B* mutations[7–13] indicate an emerging group of developmental disorders caused by aberrant histone H3 acetylation.

Subjects and Methods

Human Subjects

Families gave consent for studies approved by the CHU Sainte-Justine Institutional Review Board or by the institutional review boards of the DDD (Decipher Developmental Disorder) Study, the CAUSES (Clinical Assessment of the Utility of Sequencing and Evaluation as a Service) Study, or the Leiden University Medical Center and Maastricht University Medical Center. Written informed consent was obtained for all ten individuals involved in this study.

Exome and Sanger Sequencing

Individual P1's exome sequencing was performed as a part of the CAUSES study. Clinical exome sequencing of individual P2 was carried out at Baylor Genetics. For individual P3 (sibling of individual P2), only Sanger sequencing of a candidate mutation was done at Baylor Genetics. Clinical exome sequencing for individuals P4 and P5 was performed at GeneDx. Exome sequencing of individuals P6 and P10 was carried out at Leiden University Medical Center and Maastricht University Medical Center, respectively. Individuals P7, P8, and P9 were subject to research exome sequencing as a part of the DDD study. After exome sequencing, PCR fragments were amplified from genomic DNA or reversely transcribed cDNA to confirm *BRPF1* mutations.

Lymphoblastoid Cell Line Preparation

Lymphoblastoid cell lines were established and cultured as described previously.[30]

Animal Study Approval

Mice used were in the C57BL/6J genetic background. The *Brpf1*^{f} allele contains two loxP sites flanking exons 4–6 of *Brpf1*.[25,27,28] EIIa-Cre-mediated total knockouts, as well as forebrain-specific and hematopoietic-specific knockouts, have been described elsewhere.[26–29] To generate epiblast-specific knockouts, *Brpf1*$^{f/f}$ mice were mated with the *Meox2-Cre* strain (Jackson Laboratory, 003755; Bar Harbor). Knockout efficiency was verified by genomic PCR and/or quantitative reverse-transcription PCR (qRT-PCR) as previously described.[26–29,31] Mouse-related procedures were performed according to the Animal Use Protocol 5786, which was reviewed and approved by the Facility Animal Care Committee of McGill University.

Immunoprecipitation and Histone Acetylation Assays

An expression plasmid for FLAG-tagged KAT6A was transfected into HEK293 cells, along with expression vectors for HA-tagged BRPF1, ING5, and MEAF6, as specified. About 48 hr after transfection, cells were washed twice with PBS, and soluble protein extracts were prepared for affinity purification on anti-FLAG M2 agarose (Sigma) as previously described.[20,31] The FLAG peptide was used to elute bound proteins for immunoblotting with anti-FLAG and -HA antibodies or for acetyltransferase activity determination. Acetylation of HeLa oligonucleosomes was performed as previously reported.[20,31] After acetylation reactions, immunoblotting was carried out to detect histone H3 or its site-specific acetylation and was performed with anti-histone H3 (Abcam, ab1791), anti-H3K9ac (Abcam, ab10812), anti-H3K14ac (EMD Millipore, 07-353), anti-H3K18ac (EMD Millipore, 07-354), and anti-H3K23ac (EMD Millipore, 07-355) antibodies.

Fluorescence Microscopy

For analysis of subcellular localization, expression plasmids for EGFP-BRPF1 and its mutants were transiently transfected into HEK293 cells with or without those for KAT6A, ING5, and MEAF6, as specified in Figure S4. About 16 hr after transfection, live green fluorescence signals were examined under a fluorescence microscope, and fluorescence images were captured for further processing as previously described.[31]

qRT-PCR and Regular PCR

For analysis of nonsense-mediated mRNA decay (NMD), control and mutant lymphoblastoid cells and fibroblasts were prepared for RNA extraction. RNA was reversely transcribed with the QuantiTect Reverse Transcription Kit (QIAGEN). qRT-PCR was performed on Realplex2 (Eppendorf) with the Green-2-Go qPCR Mastermix (BioBasic). Primers were designed on the web-based IDT real-time PCR primer designer and synthesized by IDT Biotechnology. BR27 (5′-TTT CCC GAA TTC AAG CTG CCA GAG GTG GTC TA-3′) and BR20 (5′-GGG CCC AAG CTT AGT CCT CCT CGT CCA TGT C-3′) were for amplification of the region corresponding to the N-terminal part of BRPF1, whereas BR11 (5′-G GCA CGG AAG AAT TCC TGG CAG AGA A-3′) and BR10 (5′-TTT CCC AAG CTT AGCT GTG CAG CCT CTG CAT-3′) were for a region encoding the C-terminal part of BRPF1.

To determine whether NMD definitely degradates the mutated *BRPF1* transcript, cDNA prepared from fibroblasts cultured from a skin biopsy of individual P5 was used for PCR amplification with primers BR419 (5′-TTG AGC ACA TCC CAC CAG CT-3′) and BR421 (5′-TGT TCT TTA AGG GCC CAG TT-3′). The amplified fragment was gel purified for Sanger sequencing. To verify her heterozygous mutation, genomic DNA from this individual and her parents was used for PCR amplification with primers BR419 and BR420 (5′-GTG GTG GGA TGC AGG GCA CT-3′). DNA fragments were gel purified for sequencing.

Table 1. Identification of *BRPF1* Mutations in Ten Individuals

Individual	Mutation (GenBank: NM_001003694.1)	Substitution in BRPF1	Origin of Mutation
P1	c.362_363delAG	p.Glu121Glyfs*2	de novo
P2	c.942_955del	p.Trp315Leufs*26	parental samples not available; biological mother affected by intellectual disability and father by cerebral palsy
P3	c.942_955del	p.Trp315Leufs*26	
P4	c.1108C>T	p.Pro370Ser	mosaic in unaffected mother; mosaicism, 7% in blood DNA, based on exome sequencing reads (21/293)
P5	c.1363C>T	p.Arg455*	de novo
P6	c.1688_1689del	p.His563Profs*8	de novo
P7	c.1883_1886dup	p.Gln629Hisfs*34	de novo
P8	c.2497C>T	p.Arg833*	de novo
P9	c.2915dupC	p.Met973Asnfs*24	de novo
P10	c.3298C>T	p.Arg1100*	de novo

Statistical Analysis

Statistical analysis was performed with an unpaired two-tailed Student's t test. $p < 0.05$ was considered to be statistically significant. Graphs were generated with GraphPad Prism 6 (Graphpad Software).

Results

Identification and Clinical Features of Ten Subjects with *BRPF1* Mutations

Mutations in *KAT6A* and *KAT6B* have recently been discovered in dozens of individuals with intellectual disability and congenital abnormalities.[7–13] Our recent mouse genetic studies have shown that *Brpf1* is essential for embryo survival, hematopoiesis, and brain development.[25–29] Together, these new findings raise the interesting question of whether *BRPF1* mutations cause developmental anomalies. To address this question, we sought to leverage exome sequencing that had been carried out on a clinical or research basis at different institutions around the world. In addition to the use of prior collaborations, we employed new web-based matching tools such as Genematcher[32] and Decipher[33] to identify individuals with mutations in *BRPF1*. In the process, we identified ten subjects carrying nine heterozygous mutations in the gene (Table 1). These subjects were from nine different families. Seven mutations were de novo (individuals P1 and P5–P10; Table 1 and Figure S1). As for the remaining two mutations, individual P4 inherited the c.1108C>T mutation (GenBank: NM_001003694.1) from his mother, who was mosaic for the mutation (mosaicism, 7% in blood DNA; Tables 1 and S1). Individuals P2 and P3 are adopted siblings whose biological mother is affected with intellectual disability. The siblings share the same variant (c.942_955del; Tables 1 and S1), which is presumed to be maternal in origin, although their biological mother is unavailable for testing.

Global developmental delay, expressive language impairment, and intellectual disability were observed in all individuals (Tables 2 and S1). As shown in Figure 1A, facial dysmorphisms include a flat facial profile, a round face, a broad root of the nose, widely spaced eyes (with downslanting palpebral fissures), ptosis, and blepharophimosis. A majority of the ten individuals have hypotonia and gross and fine motor delay. Five of them had neonatal feeding issues. Four have epilepsy. In addition, one individual had episodes of staring spells consistent with absence seizures, but electroencephalogram (EEG) only showed high voltage hypnogogic hypersynchrony, without epileptiform activity (Tables 1 and S1). Another individual displayed EEG abnormalities when treated with oxcarbazepine, but did not have clinical seizures (Tables 1 and S1). Some individuals had MRI anomalies; two had white matter hyper-intensity and two had a paucity of white matter, including thinning of the corpus callosum in one of them (Figure 1B and Table 2). These results suggest abnormal myelination in patients with *BRPF1* mutations. Interestingly, myelination and corpus callosum defects are present in forebrain-specific *Brpf1*-knockout mice.[28] Three individuals also displayed C2-C3 spinal fusions (Table S1), which is consistent with deregulated *Hox* expression upon *Brpf1* deletion in mice[28] and with skeletal abnormalities in *Brpf1*-null zebrafish.[24] Additional dysmorphisms, malformations, and clinical issues in the ten individuals are detailed in Table S1.

BRPF1 Mutations Are Predicted to Generate Different Types of Variants

Among the *BRPF1* mutations, one is missense and the remaining eight are nonsense mutations or reading frameshifts that lead to C-terminal truncations of the protein (Table 1 and Figure 2A). The missense mutation in individual P4 (p.Pro370Ser [c.1108C>T]; Table 1 and Figure 2A) alters the codon for Pro370, which is invariant from *Drosophila* to humans (Figure 2B) and is located within a loop of the PZP domain important for non-specific binding to the DNA backbone of nucleosomes (Figure 2C).[23] Moreover, it is almost invariant in PZP domains from nine other human proteins, including three JADE proteins, three histone demethylases, and three zinc finger proteins

Table 2. Summary of Major Clinical Features in Ten Individuals with *BRPF1* Mutations

	P1	P2	P3	P4	P5	P6	P7	P8	P9	P10
Neonatal feeding difficulties	N	Y	NA	Y	N	N	Y	N	N	Y
Hypotonia	Y	Y	NA	Y	Y	Y	NA	N	Y	Y
Gross motor delay	Y	Y	Y	Y	Y	Y	Y	N	Y	Y
Fine motor delay	Y	Y	Y	N	Y	N	U	Y	Y	U
Language delay	Y	Y	Y	Y	Y	Y	Y	Y	Y	Y
GDD or ID	Y	Y	Y	Y	Y	Y	Y	Y	Y	Y
Epilepsy	N	Y	Y	EEG anomaly	probable absence seizures	N	Y	N	Y	N
Brain MRI	WM hyper-intensity	decreased WM and thin CC	nl	nl	nl	NA	NA	NA	decreased WM	nl
Flat facial profile	Y	N	Y	Y	Y	N	U	Y	Y	Y
Round face	Y	Y	Y	N	Y	N	Y	Y	N	Y
Broad root of the nose	Y	Y	Y	Y	Y	N	Y	Y	Y	Y
Widely spaced eyes	Y	Y	Y	Y	Y	N	Y	Y	Y	Y
Down-slanting palpebral fissures	N	Y	N	N	N	N	Y	N	Y	Y
Ptosis	Y	N	Y	N	Y	Y	Y	N	N	Y
Blepharophimosis	U	N	Y	Y	Y	N	NA	N	N	Y
Spinal anomalies	Y	Y	Y	N	Y	NA	NA	N	N	NA
Joint hypermobility	Y	N	N	N	Y	Y	Y	Y	Y	N

See Table S1 for more details. Abbreviations are as follows: CC, corpus callosum; GDD, global developmental delay; ID, intellectual disability; N, no; NA, data not available, nl, normal; U, unknown; WM, white brain matter; Y, yes.

(AF-10, AF-17, and PHF14) (Figure S2). All eight truncating mutations encode variants lacking important structural domains of BRPF1 (Figure 2A). The variants p.Glu121Glyfs*2 (c.362_363delAG) (individual P1; Table 1), p.Trp315Leufs*26 (c.942_955del) (individuals P2 and P3), p.Arg455* (c.1363C>T) (individual P5), and p.His563Profs*8 (c.1688-1689del) (individual P6) are devoid of the ING5- and MEAF6-interacting domain (Figure 2A). On the basis of published data,[20] these variants are predicted to be unable to form tetrameric complexes with KAT6A (or KAT6B), ING5, and MEAF6. By contrast, the ING5- and MEAF6-interacting domain is intact in the remaining four truncation variants, p.Gln629Hisfs*34 (c.1883_1886dup), p.Arg833* (c.2497C>T), p.Met973Asnfs*24 (c.2915dupC), and p.Arg1100* (c.3298C>T) (individuals P7–P10, respectively; Table 1 and Figure 2A). These four mutants are expected to form tetrameric complexes with KAT6A (or KAT6B), ING5, and MEAF6. Therefore, the nine mutations appear to generate three distinct groups of variants, suggesting that the mutations might deregulate BRPF1 functions through different mechanisms.

BRPF1 Loss Reduces Histone H3K23 Acetylation In Vivo

Through the EPC-like motif N-terminal to the PZP domain and a conserved region further N-terminal to this motif, BRPF1 interacts with and activates three histone acetyltransferases, KAT6A, KAT6B, and KAT7.[19–21] *Drosophila* Enok (a fly acetyltransferase with a catalytic domain highly homologous to those of KAT6A and KAT6B) and Br140 (orthologous to BRPF1) are crucial for histone H3K23 acetylation.[38,39] We found that BRPF1 is also important for histone H3K23 acetylation in the mouse bone marrow.[29] In agreement with this, H3K23 acetylation was defective in thymus and spleen protein extracts from hematopoietic-specific *Brpf1*- knockout pups (Figures 3A and 3B). Moreover, similar defects were present in dorsal cortex extracts of forebrain-specific *Brpf1*-knockout pups (Figure 3C) and protein extracts of epiblast-specific *Brpf1*-knockout embryos (Figure 3D, lanes 1 and 4–6). Interestingly, heterozygous mutant embryos also displayed reduced H3K23 acetylation (Figures 3D and 3E, compare lanes 1–3), which is relevant to monoallelic mutations in the ten individuals (Table 1). Furthermore, H3K23 acetylation was not detectable in *Brpf1*$^{-/-}$ mouse embryonic fibroblasts (Figure 3F). By contrast, histone H3K9 and H3K14 acetylation was less consistently affected in different *Brpf1*-knockout samples (Figures 3A–3F). Therefore, mouse Brpf1 governs H3K23 acetylation in different tissues and cells in vivo.

These results prompted us to investigate whether histone H3K23 acetylation is affected in cells from individuals with *BRPF1* mutations. Lymphoblastoid cells from individual P4 (p.Pro370Ser; Table 1) showed reduced

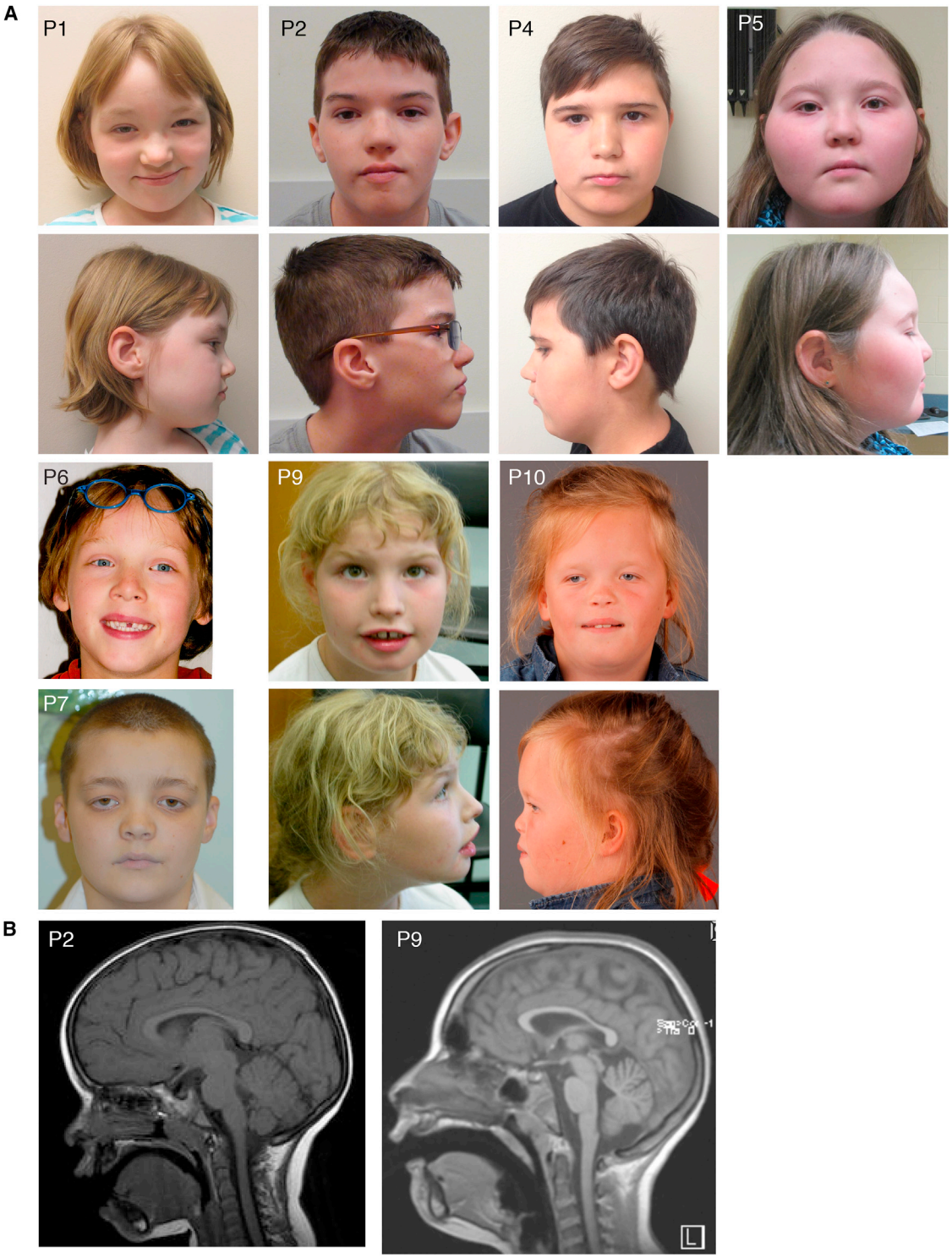

Figure 1. Facial and Brain Characteristics of Individuals with *BRPF1* Mutations
(A) Photos for eight individuals. The photos are not in the same scale. Ages of the individuals when the photos were taken are as follows: P1, 6 years and 5 months; P2, 13 years and 3 months; P4, 10 years and 6 months; P5, 8 years and 3 months; P6, 4 years; P7, 12 years and 6 months; P9, 8 years; P10, 12 years.
(B) Brain magnetic resonance imaging (MRI) images of individuals P2 and P9.

H3K23 acetylation (~50% of the control; Figure 3G). In comparison, qRT-PCR revealed no decrease in the amount of *BRPF1* mRNA in mutant cells (Figure S3A). We also obtained a skin biopsy from individual P5 (p.Arg455*; Table 1) for preparation of fibroblasts. As shown in Figure 3H, H3K23 acetylation in the fibroblasts also decreased to ~50% of the control. These results indicate that two mutations lead to decreased H3K23 acetylation

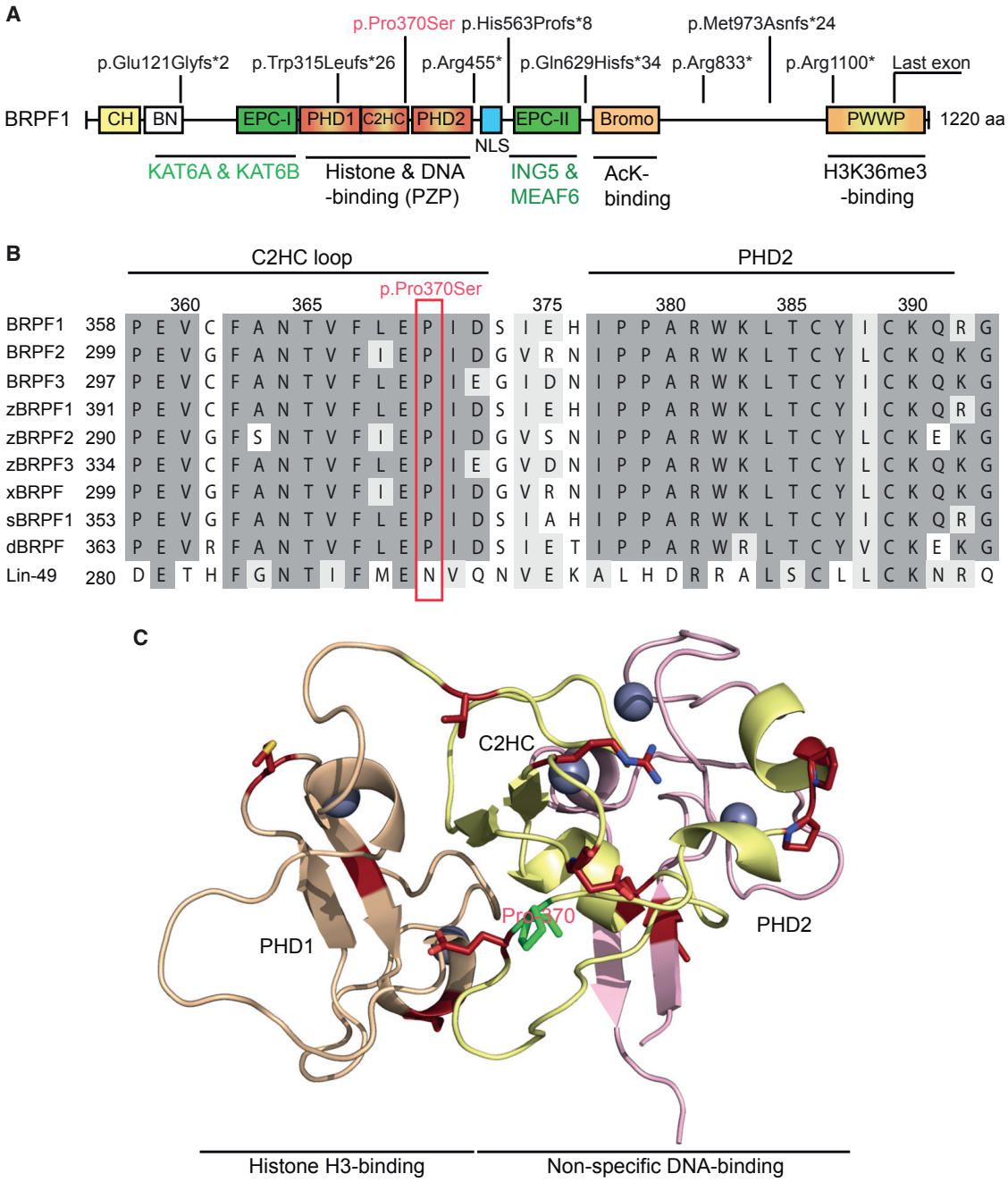

Figure 2. Domain Organization of BRPF1 and Its Variants from Individuals with Developmental Anomalies

(A) Schematic representation of BRPF1 and nine variants as identified in ten individuals. See Table 1 for DNA sequence changes in the individuals. BRPF1 possesses multiple modules, including the PZP domain, bromodomain, and PWWP domain, for chromatin association. The PZP domain comprises two PHD fingers linked with a C2HC zinc finger. The first PHD finger recognizes the N terminus of histone H3.[21,23,34] The C2HC zinc knuckle and the second PHD finger form a non-specific DNA binding domain.[22,23] The bromodomain has acetyllysine-binding ability,[35] and the PWWP domain targets trimethylated histone H3.[36,37] The EPC-like motif C-terminal to the PZP domain is essential for formation of a stable trimeric complex with ING5 and MEAF6.[19–21] Through the EPC-like motif N-terminal to the PZP domain and a conserved region further N-terminal to this motif, BRPF1 interacts with and activates KAT6A, KAT6B, and KAT7.[19–21] Unlike p.Pro370Ser, the other eight variants contain C-terminal truncations due to nonsense or reading-frameshift mutations. These mutations are not located within the last coding exon and might trigger NMD in vivo. Abbreviations are as follows: CH, C2H2 zinc finger; BN, conserved BRPF N-terminal domain; EPC, enhancer of polycomb-like motif; NLS, nuclear localization signal.

(B) Sequence alignment of human BRPF1 with its paralogs (BRPF2 and BRPF3), as well as the orthologs from zebrafish (z), *Xenopus* (x), sea urchin (s), *Drosophila* (d), and *C. elegans* (Lin-49). There is one ortholog per organism from the worm to *Xenopus*, but there are three in zebrafish. Pro370 of BRPF1 and its corresponding residues in its paralogs and orthologs are boxed in red.

(C) Pro370 is located within a loop connecting the C2HC knuckle to the second PHD finger. PHD1 recognizes the free N terminus of histone H3,[21,23,34] whereas the C2HC zinc knuckle and PHD2 form a module for non-specific interaction with the DNA backbone of the nucleosome.[23] The structural model was generated based on a published report,[23] with kind help of Tatiana G. Kutateladze.

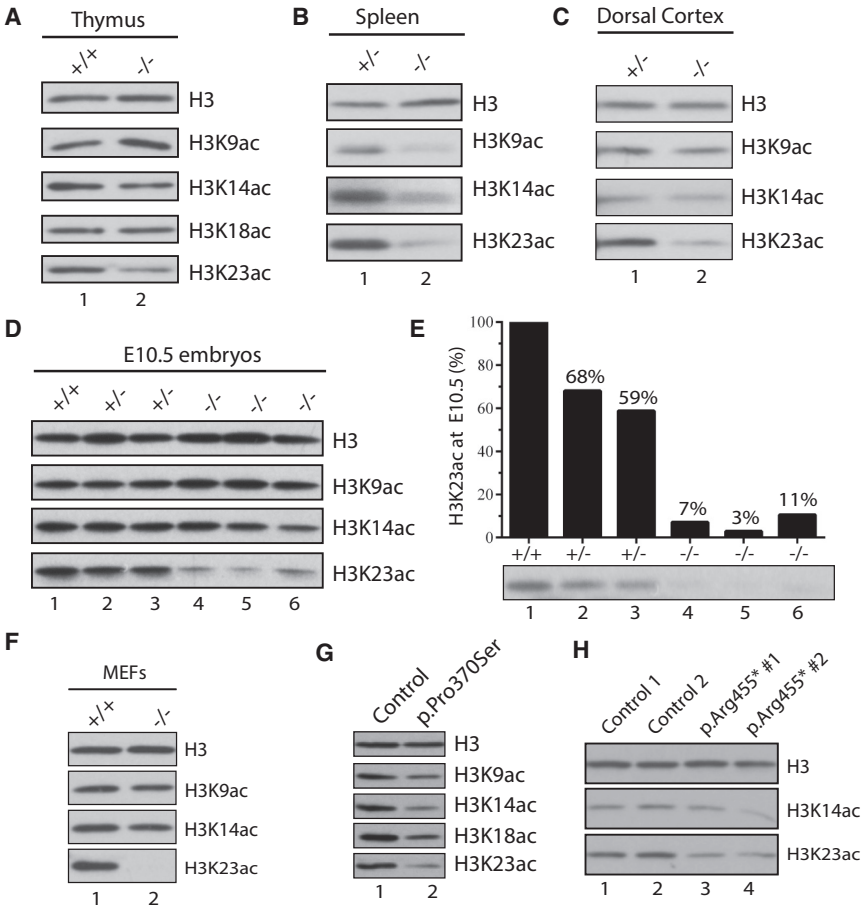

Figure 3. BRPF1 Loss Reduces Histone H3K23 Acetylation In Vivo

(A and B) Histone H3 acetylation in thymus and spleen protein extracts from control and hematopoietic-specific *Brpf1*-knockout mice.

(C) Histone H3 acetylation in dorsal cortical extracts from heterozygous and forebrain-specific *Brpf1* knockouts.

(D) Histone H3 acetylation in protein extracts from wild-type and epiblast-specific *Brpf1*-knockout embryos at embryonic day 10.5 (E10.5).

(E) Quantification of H3K23 acetylation in proteins extracts from wild-type and epiblast-specific *Brpf1* knockout embryos at E10.5. The blot was from the same experiment as shown in (D), but the exposure time was shorter than the bottom image in (D). The quantification was performed with NIH ImageJ.

(F) Histone H3 acetylation in protein extracts from control and *Brpf1*-knockout mouse embryonic fibroblasts (MEFs). The fibroblasts were prepared from control and tamoxifen-inducible knockout embryos at E15.5.[27]

(G) Histone H3 acetylation in protein extracts from control and p.Pro370Ser lymphoblastoid cells.

(H) Histone H3 acetylation in protein extracts from control and p.Arg455* fibroblasts.

in individuals P4 and P5 (Table 1 and Figures 3G and 3H). Consistent with this, RNAi knockdown showed that BRPF1 is important for H3K23 acetylation in human U2OS cells.[40]

NMD degradates a premature stop codon-containing transcript expressed in *Brpf1*-knockout mice.[26,28,29] The mutation in individual P5 introduces a stop codon in a middle exon (Figure 2A) and might thus trigger NMD. To investigate this, we first performed qRT-PCR to analyze *BRPF1* mRNA amounts in the control and mutant fibroblasts. One primer set, but not the other, detected some decrease of *BRPF1* mRNA in the mutant cells (Figure S3B). To resolve this difference, cDNA from the mutant fibroblasts was prepared and sequenced. The results revealed that the wild-type and mutant alleles were similarly expressed (Figure S1C), indicating that NMD is not at play with the mutant transcript in fibroblasts from individual P5. To substantiate this, we compared lymphoblastoid cells from this individual and her parents. qRT-PCR analysis of *BRPF1* mRNA detected no difference between the mutant and control cells (Figure S3C). Furthermore, we analyzed lymphoblastoid cells from individual P2, also carrying a premature stop codon in the mutant allele (Table 1). qRT-PCR analysis of *BRPF1* mRNA detected no difference between the mutant and control cells (Figure S3D). Together, these results suggest that NMD does not apply to the mutant transcripts in individuals P2 and P5. Notably, a similar conclusion has been reached for *KAT6A* and *KAT6B* mutations.[9,12]

Impact of *BRPF1* Mutations on Histone H3K23 Acetylation In Vitro

To delineate further the molecular mechanisms by which the *BRPF1* mutations affect H3K23 acetylation, we engineered seven variants encoded by the mutations and analyzed the impact on formation of tetrameric complexes with KAT6A (Figure 4). The variants were produced transiently in HEK293 cells with KAT6A, ING5, and MEAF6 for co-immunoprecipitation. BRPF1 serves as a scaffold protein to bridge interaction of KAT6A and KAT6B with ING5 and MEAF6.[19,20] Exogenous BRPF1 promoted production of ING5 and MEAF6 (Figure 4A, top panel, lanes 1 and 2). We observed similar effects with p.Pro370Ser, p.Gln629Hisfs*34, p.Arg833*, and p.Arg1100* (Figures 4A, 4C, and 4D, top panels). Moreover, like wild-type BRPF1, these four variants form tetrameric complexes with KAT6A, ING5, and MEAF6 (Figures 4A, lanes 2 and 3, and 4D, lanes 4–7). By contrast, p.Glu121Glyfs*2, p.Trp315Leufs*26, and p.Arg455* failed to promote expression of ING5 and MEAF6 (Figures 4C and 4D, top panel). p.Glu121Glyfs*2 was not produced as well as the wild-type (Figure 4C, top panel) and failed to interact with

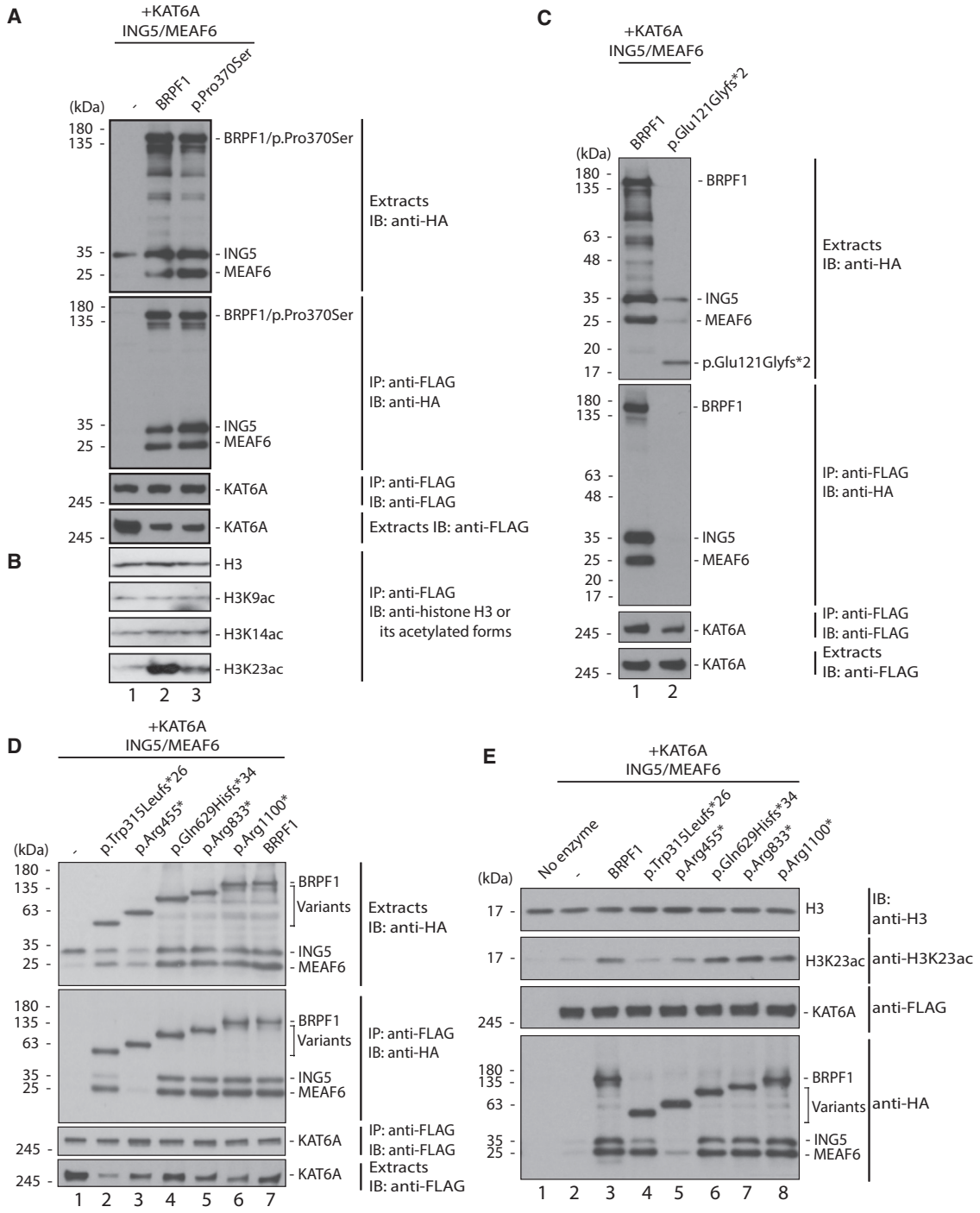

Figure 4. Functional Characterization of BRPF1 Variants In Vitro

(A) Interaction of BRPF1 and the variants with KAT6A, ING5, and MEAF6. KAT6A was produced in HEK293 cells as a FLAG-tagged fusion protein along with HA-tagged BRPF1 (or the p.Pro370Ser variant), ING5, and MEAF6 as indicated. Soluble protein extracts were prepared for affinity purification on anti-FLAG agarose, and bound proteins were eluted with the FLAG peptide for immunoblotting with anti-FLAG and -HA antibodies.

(B) Histone acetylation assays. HeLa oligonucleosomes were used as substrates for acetylation by proteins affinity purified in (A). Acetylation of histone H3 was detected with antibodies recognizing histone H3 and its acetylated forms as indicated.

(C and D) Same as (A) except that different BRPF1 variants were analyzed. Unexpectedly, the variant p.Trp315Leufs*26 still showed strong interaction with MEAF6; whether this is due to the extra 26 residues introduced after the reading frameshift remains unclear.

(E) Histone acetylation assays. Proteins affinity-purified in (D) were used for the enzymatic assays as in (B).

KAT6A to form a tetrameric complex with ING5 and MEAF6 (Figure 4C). The remaining two variants interacted with KAT6A similarly to wild-type BRPF1 (Figure 4D, lanes 1–3 and 7). As expected, given its lack of the ING5- and MEAF6-interacting domain (Figure 2A), p.Arg455* failed to mediate the interaction of KAT6A with ING5 and

MEAF6 (Figure 4D, lanes 3 and 7). Unexpectedly, pTrp315Leufs*26 was still able to interact with MEAF6 (compare lanes 2 and 7). Whether this is due to the extra 26 residues introduced by the reading frameshift remains unclear. These results support that the nine variants (Table 1 and Figure 2A) form different groups according to the ability to form tetrameric complexes with KAT6A, ING5, and MEAF6.

We next investigated whether the BRPF1 variants stimulate the acetyltransferase activity of KAT6A. As shown in Figure 4B (lanes 1 and 2), wild-type BRPF1 promoted H3K23 acetylation by KAT6A when oligonucleosomes were used as the substrate. By contrast, p.Pro370Ser failed to do so (Figure 4B, lanes 1–3). This is consistent with reduced H3K23 acetylation in lymphoblastoid cells prepared from individual P4 (Figure 3G). These results attest to the importance of the DNA-binding loop of BRPF1 in regulating the acetyltransferase activity of KAT6A. Like this mutant, the variant pTrp315Leufs*26 was inactive in stimulating the acetyltransferase activity of KAT6A (Figure 4E, lanes 1–4). The variant p.Arg455* showed reduced ability to stimulate the acetyltransferase activity of KAT6A (compare lanes 1–3 and 5). The impaired ability of the variants pTrp315Leufs*26 and p.Arg455* is likely due to the loss of the domain crucial for ING5 and EAF6 interaction (Figure 1A).[20] By contrast, p.Gln629Hisfs*34, p.Arg833*, and p.Arg1100* were as active as wild-type BRPF1 in stimulating the acetyltransferase activity of KAT6A (Figure 4E, lanes 6–8), in agreement with their ability to form tetrameric complexes with KAT6A, ING5, and MEAF6, similarly to wild-type BRPF1 (Figure 4D, lanes 4–7). The variants p.Arg833* and p.Arg1100* lack the PWWP domain, which binds to trimethylated histone H3 in vitro.[36,37] Moreover, a mutant lacking this domain causes developmental defects in zebrafish.[24] Thus, the findings on these two variants reiterate the importance of the PWWP domain in vivo.

We also analyzed subcellular localization of BRPF1 and its mutants by fluorescence microscopy. As reported for NIH 3T3 fibroblasts,[20] when produced alone in HEK293 cells, BRPF1 formed cytoplasmic dots but became more nuclear with co-production of KAT6A, ING5, and MEAF6 (Figure S4). By themselves, p.Glu121Glyfs*2 and p.Trp315Leufs*26 presented uniform cytoplasmic distribution, whereas p.Arg455* and p.Gln629Hisfs*34 were mainly nuclear (Figure S4). In the presence of exogenous KAT6A, ING5, and MEAF6, these four variants were all nuclear (Figure S4). The variant p.Arg833* formed large aggregates in the cytoplasm but became nuclear upon co-production of KAT6A, ING5, and MEAF6 (Figure S4). By itself, the missense variant p.Pro370Ser showed cytoplasmic distribution different from the wild-type but translocated to the nucleus upon co-production of KAT6A, ING5, and MEAF6 (Figure S4). Thus, the missense and truncation variants all behaved differently from wild-type BRPF1 (Figure S4). Together, results from determination of enzymatic activity (Figures 3 and 4) and subcellular localization (Figure S4) support that the *BRPF1* mutations lead to pathogenicity through different mechanisms.

Distribution of Histone H3K23 Acetylation in the Mouse Brain

Intellectual disability in the individuals with *BRPF1* mutations (Tables 1, 2, and S1) suggests the importance of BRPF1 in human brain development. In support of this, *BRPF1* was highly expressed in the brain,[25] and forebrain-specific inactivation of mouse *Brpf1* leads to defects in the cerebrum and hippocampus.[26,28] In addition, mouse *Kat6b* is important for cerebral development.[41] We thus analyzed distribution of H3K23 acetylation in the mouse brain. For this, indirect immunofluorescence microscopy was performed on mouse brain sections. As shown in Figure 5, fluorescence signals for H3K23 acetylation were detectable in the cerebral cortex but enhanced in the hippocampus and cerebellum. In the hippocampus, the signal was enriched within *Cornu Ammonis* areas and the dentate gyrus (Figure 5). In addition, the signals were high at islands of Calleja located within the olfactory tubercle (Figure 5). The cerebrum, hippocampus, and olfactory tubercle are all important for learning and memory. Moreover, the H3K23ac distribution is very similar to the expression pattern of mouse *Brpf1* in the brain, as determined with a knockin reporter.[25] These results further support that BRPF1 acts through H3K23 acetylation to regulate brain functions.

BRPF1 Governs H3K23 Acetylation through KAT6A and KAT6B

Via the EPC-like motif N-terminal to the PZP domain and a conserved region further N-terminal to this motif (Figure 2A), mammalian BRPF1 interacts with three histone acetyltransferases, KAT6A, KAT6B, and KAT7.[19–21] Although *Drosophila* Br140 co-purified efficiently with Enok (homologous to KAT6A and KAT6B), Chameau (orthologous to KAT7) was not detectable.[38,39,42] An interesting question is how KAT6A, KAT6B, and KAT7 contribute to BRPF1 functions in mammals. The binding sites for these KATs are all located within the N-terminal domain of BRPF1,[19–21] so we investigated its competitive interaction with KAT6A and KAT7. For this, BRPF1 was produced in HEK293 cells as a FLAG-tagged fusion protein along with HA-tagged KAT6A (or KAT7), ING5, and MEAF6, as indicated (Figure 6A). Soluble protein extracts were prepared for co-immunoprecipitation. As shown in Figure 6A, the MYST domain of KAT6A formed an almost stoichiometric complex with ING5 and MEAF6, whereas the amount of KAT7 co-precipitated with BRPF1 was much lower (compare lanes 4 and 6). When both acetyltransferases were produced together (lane 5), competition was not obvious, supporting that they utilize distinct binding sites. Related to this, KAT7 binds to the BN domain of BRPF1,[21] whereas KAT6A binds to a region more C-terminal to the BN domain (Figure 4).[20] Based on the amount of KAT7 recovered from co-immunoprecipitation

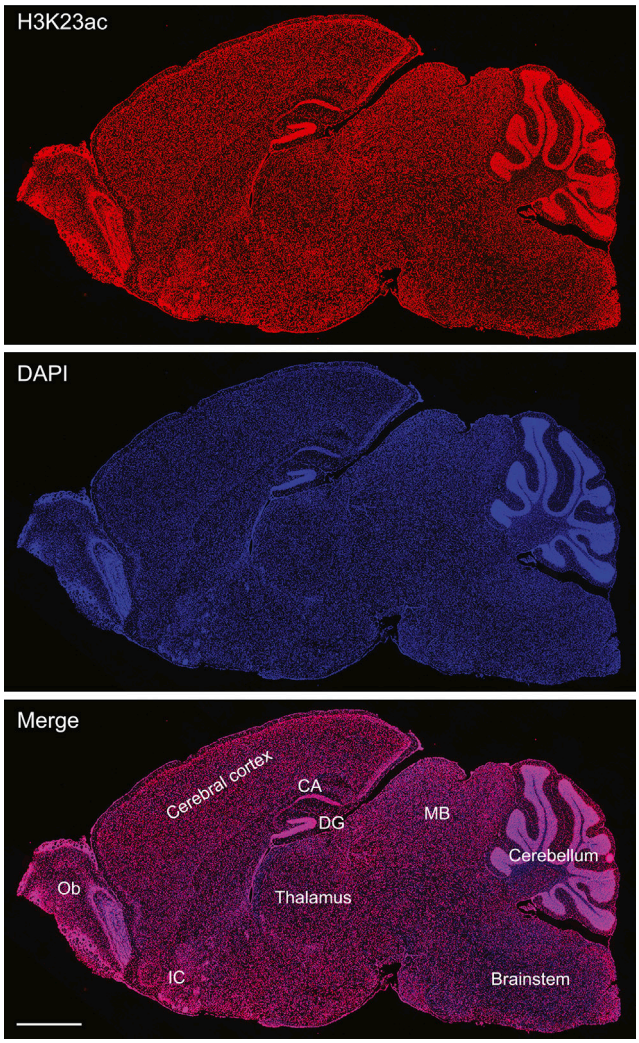

Figure 5. Distribution of Histone H3K23 Acetylation in the Mouse Brain

Adult mouse brain sections were used for indirect immunofluorescence microscopy with the anti-H3K23ac antibody (upper), with nuclei counterstained with DAPI (middle). H3K23ac signals are enriched in the hippocampus, cerebellum, olfactory bulb (OB), and islands of Calleja (IC). Within the hippocampus, the fluorescence signals were high in Cornu Ammonis (CA) areas and the dentate gyrus (DG). Images of one representative parasagittal brain section are shown here. MB, mid-brain. Scale bar, 1 mm.

(Figure 6A), its binding to BRPF1 appeared to be much weaker than that of KAT6A. KAT6A is paralogous to KAT6B,[20,43] so these results suggest that BRPF1 mainly acts through KAT6A and KAT6B to control H3K23 acetylation in vivo (Figure 6B, left). These results also imply that through altering H3K23 acetylation by these two acetyltransferases, *BRPF1* mutations cause developmental anomalies (Figure 6B, right).

Discussion

Chromatin structure and function constitute an integral component of epigenetic regulation. To interpret different chromatin modification states, the human genome encodes several hundred chromatin readers. Some of them have been investigated at the molecular level and in model organisms, but very few have been associated with Mendelian disorders in humans. Results presented herein show that *BRPF1* mutations cause a developmental disorder in ten individuals with an intellectual disability syndrome (Figures 1 and 2 and Table 2). Developmental delay, intellectual disability, and language impairment are consistent with recent knockout studies showing that mouse *Brpf1* is critical for embryo survival and forebrain development.[26–28] The individuals are heterozygous for the mutations (Figures 1 and 2A). The mutated alleles are not functional in individuals P1–P5, P7, and P8 (Figures 3, 4, and S4), and perhaps also in individuals P6, P9, and P10 (Tables 1), so haploinsufficiency might be the pathological mechanism, as observed in several developmental disorders due to *KAT6A* mutations or *KAT6B* mutations.[7–13] Some clinical features such as intellectual disability and developmental delay reported herein are common to those in persons with *KAT6A* or *KAT6B* mutations,[7–13] but craniofacial dysmorphisms are less striking in individuals with *BRPF1* mutations (Figure 1 and Table 2). Although the number of patients is not large enough to draw broad conclusions, most individuals with *BRPF1* variants do not exhibit microcephaly, as seen in persons with *KAT6A* variants,[12,13] or possess genital and patellar abnormalities observed in genitopatellar syndrome (MIM: 606170) due to *KAT6B* mutations.[9,10] However, clinical variability has been observed in persons with *KAT6B* variants, which can present as genitopatellar syndrome or the Say-Barber-Biesecker-Young-Simpson variant of Ohdo syndrome (MIM: 603736).[7–11] Notably, a majority of *KAT6A* and *KAT6B* mutations remove the serine- and methionine-rich transcriptional activation domain but leave the acetyltransferase domain intact,[7–13] so they are not expected to affect global histone H3K23 acetylation per se. This is different from the major impact of *BRPF1* mutations on histone H3K23 acetylation (Figures 2–4), raising a therapeutic prospect whereby it might be beneficial to correct this deficiency with deacetylase inhibitors.

Molecular analyses showed that the mutations impair H3K23 acetylation (Figure 3) due to defects in activating the acetyltransferases KAT6A and KAT6B (Figure 4) and in maintaining proper subcellular distribution (Figure S4). The latter is especially important for those variants lacking the PWWP domain only (Figure 2A). Moreover, it has been shown that the PWWP domain is important both in vitro and in vivo.[24,36,37] For H3K23 acetylation, BRPF1 acts predominantly through KAT6A and KAT6B (Figure 6A). These molecular results are consistent with two recent reports showing that BRPF1 is important for histone H3K23 acetylation in mouse hematopoietic stem cells and that KAT6B is a histone H3K23 acetyltransferase in lung cancer cells.[29,44] Moreover, *Drosophila* Enok and Br140 are crucial for histone H3K23 acetylation.[38,39] Together, these studies suggest that BRPF1 acts through

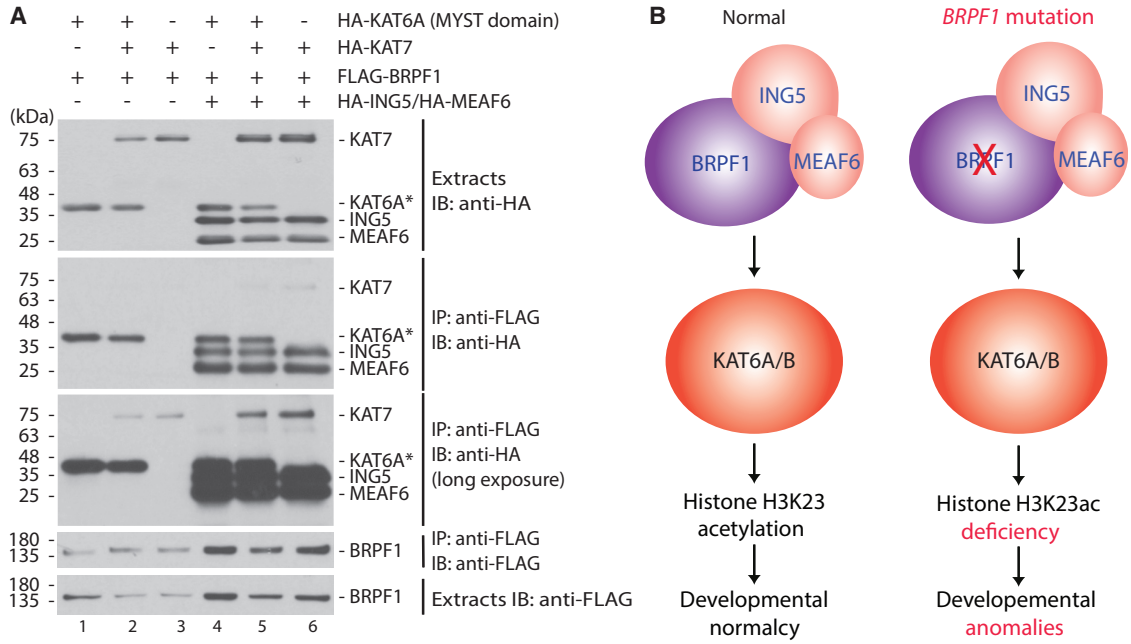

Figure 6. BRPF1 Governs H3K23 Acetylation through KAT6A and KAT6B

(A) Competitive interaction of BRPF1 with KAT6A and KAT7. BRPF1 was produced in HEK293 cells as a FLAG-tagged fusion protein along with HA-tagged KAT6A (or KAT7), ING5, and MEAF6 as indicated. For KAT6A, only its MYST domain was produced (labeled as KAT6A*). Soluble protein extracts were prepared for affinity purification on anti-FLAG agarose, and bound proteins were eluted with the FLAG peptide for immunoblotting with anti-FLAG and -HA antibodies.

(B) Cartoon showing how *BRPF1* mutations affect histone H3K23 acetylation and cause developmental abnormalities. In individuals without *BRPF1* mutations (left), BRPF1 forms a trimeric complex with ING5 and EAF6 to control histone H3K23 acetylation by KAT6A and KAT6B, which in turn regulate developmental programs. In individuals with *BRPF1* mutations (right), BRPF1 variants fail to exert proper control on histone H3K23 acetylation, thereby deregulating normal gene expression and developmental programs. For simplicity, the cartoon does not illustrate additional partners that BRPF1 might have in vivo.

KAT6A and KAT6B to govern H3K23 acetylation and that mutations in *BRPF1* might deregulate related epigenetic and developmental programs (Figure 6B).

Compared to other histone acetylation sites (such as H3K9, H3K14, H3K27, and H4K16), H3K23 is not as well characterized. However, three recent studies have unexpectedly revealed that acetylation at this site is highly abundant from *C. elegans* to humans,[45–47] suggesting evolutionarily conserved importance in different organisms. At the mechanistic level, H3K23 acetylation serves as a docking site for the chromatin reader TRIM24 in breast cancer.[48] This epigenetic mark also competes with H3K23 methylation and ubiquitination, both of which have recently emerged as two important epigenetic marks.[49,50] H3K23 acetylation might even interplay with H3K18 acetylation and H3K27 methylation, given the physical proximity to these two modification sites. Furthermore, a recent study has linked H3K23 acetylation to DNA replication and perhaps also DNA repair in *Drosophila*.[39] Thus, defective H3K23 acetylation in individuals with *BRPF1* mutations might exert polytrophic effects on molecular and cellular processes underlying the developmental anomalies.

BRPF1 is conserved from worms to humans.[51] Lin-49, a related protein in *C. elegans*, regulates neuron asymmetry, hindgut development, and fecundity.[52] *Drosophila* Br140 is highly homologous to mammalian BRPF1 and forms a tetrameric complex with Enok (homologous to KAT6A and KAT6B) to target histone H3K23 acetylation.[39,42] Enok is critical for neuroblast proliferation in the fly brain.[53] Both Br140 and Enok are important for neuronal wiring of the fly visual system too.[54] Although their functions in the nervous system remain unclear, both *Brpf1* and *Kat6a* are important for maintaining pharyngeal segmental identity and skeletal development in zebrafish.[24,55] Both *Brpf1* and *Kat6b* are critical for mouse brain development.[26,28,41] Consistent with this, intellectual disability is a major clinical feature in individuals with mutations in *BRPF1* (Table 2) or *KAT6B*.[7–11] Although the individuals described herein carry monoallelic mutations, no obvious phenotypes have been observed for heterozygous *Brpf1* mice.[24–29] Similarly, although monoallelic mutations in *KAT6A* or *KAT6B* cause developmental anomalies, no obvious phenotypes have been reported for heterozygous *Kat6a* or *Kat6b* mice.[41,56,57] We have recently found that *Brpf1* is critical for mouse hematopoietic stem cells and that its inactivation leads to pre-weaning lethality as a result of acute bone-marrow failure,[29] but no hematological abnormalities have been observed in the individuals with *BRPF1* mutations (Tables 2 and S1). Similarly, mouse *Kat6a* is critical for hematopoietic stem cells,[56,57] but no hematological abnormalities have been discovered

in patients with the *KAT6A* mutations. One major difference is that both alleles are inactivated in knockout mice but only one allele is affected in individuals with *BRPF1* or *KAT6A* mutations. In addition, over 100 missense and truncating somatic mutations in *BRPF1* have been identified in different types of cancer.[23,51] About one third of these mutations are predicted to inactivate BRPF1 functions, but no indications of cancer predisposition are present in the ten individuals with *BRPF1* mutations, although the oldest is now only 17 years old (Tables 2 and S1). Thus, further studies are needed to investigate these interesting issues.

In summary, we provide evidence that heterozygous *BRPF1* mutations cause intellectual disability and other anomalies. The mutations affect physical and functional interactions of BRPF1 with KAT6A and KAT6B, resulting in deficient histone H3K23 acetylation (Figure 6B). Our findings provide a basis for phenotypic and molecular diagnosis of the developmental disorder with *BRPF1* mutations, highlight the importance of this chromatin regulator in human development, and shed light on functions of its orthologs in different organisms. The findings also suggest potential value to using *Brpf1* mutant mice as preclinical models for exploring treatment options. This study on *BRPF1* mutations and the recent reports[7–13] on *KAT6A* and *KAT6B* mutations uncover an emerging group of intellectual disability disorders caused by aberrant histone H3 acetylation.

Supplemental Data

Supplemental Data include four figures and one table and can be found with this article online at http://dx.doi.org/10.1016/j.ajhg.2016.11.011.

Consortia

The members of the CAUSES Study consortium are Shelin Adam, Christele Du Souich, Jane Gillis, Alison Elliott, Anna Lehman, Jill Mwenifumbo, Tanya Nelson, Clara Van Karnebeek, and Jan Friedman.

Acknowledgments

This project was supported in part by operating grants from the Canadian Institutes of Health Research (RN324373 and RN315908 to P.M.C. and MOP-142252 X.J.Y.) and the Natural Sciences and Engineering Research Council of Canada (342146-12 to X.J.Y.). Funding for the CAUSES Study was from Mining for Miracles, British Columbia Hospital Foundation. The DDD Study presents independent research commissioned by the Health Innovation Challenge Fund (grant no. HICF-1009-003), a parallel funding partnership between the Wellcome Trust and the UK Department of Health, and the Wellcome Trust Sanger Institute (grant no. WT098051). The views expressed in this publication are those of the author(s) and not necessarily those of the Wellcome Trust or the Department of Health. The study has UK Research Ethics Committee (REC) approval (10/H0305/83, granted by the Cambridge South REC, and GEN/284/12, granted by the Republic of Ireland REC). The research team acknowledges the support of the National Institute for Health Research, through the Comprehensive Clinical Research Network. M.G., B.B. and M.T.C. are employees of GeneDx.

Received: August 16, 2016
Accepted: November 10, 2016
Published: December 8, 2016

Web Resources

BLAST, http://blast.ncbi.nlm.nih.gov/Blast.cgi
cBioPortal for Cancer Genomics, http://www.cbioportal.org/index.do
COSMIC, http://cancer.sanger.ac.uk/cosmic
DECIPHER, http://decipher.sanger.ac.uk/
ExAC Browser, http://exac.broadinstitute.org/
GenBank, http://www.ncbi.nlm.nih.gov/genbank/
GeneMatcher, https://genematcher.org/
OMIM, http://www.omim.org/
UCSC Genome Browser, http://genome.ucsc.edu

References

1. Li, B., Carey, M., and Workman, J.L. (2007). The role of chromatin during transcription. Cell *128*, 707–719.
2. Kouzarides, T. (2007). Chromatin modifications and their function. Cell *128*, 693–705.
3. Allis, C.D., and Jenuwein, T. (2016). The molecular hallmarks of epigenetic control. Nat. Rev. Genet. *17*, 487–500.
4. Berdasco, M., and Esteller, M. (2013). Genetic syndromes caused by mutations in epigenetic genes. Hum. Genet. *132*, 359–383.
5. Bernier, R., Golzio, C., Xiong, B., Stessman, H.A., Coe, B.P., Penn, O., Witherspoon, K., Gerdts, J., Baker, C., Vulto-van Silfhout, A.T., et al. (2014). Disruptive CHD8 mutations define a subtype of autism early in development. Cell *158*, 263–276.
6. Weiss, K., Terhal, P.A., Cohen, L., Bruccoleri, M., Irving, M., Martinez, A.F., Rosenfeld, J.A., Machol, K., Yang, Y., Liu, P., et al.; DDD Study (2016). De Novo Mutations in CHD4, an ATP-Dependent Chromatin Remodeler Gene, Cause an Intellectual Disability Syndrome with Distinctive Dysmorphisms. Am. J. Hum. Genet. *99*, 934–941.
7. Kraft, M., Cirstea, I.C., Voss, A.K., Thomas, T., Goehring, I., Sheikh, B.N., Gordon, L., Scott, H., Smyth, G.K., Ahmadian, M.R., et al. (2011). Disruption of the histone acetyltransferase MYST4 leads to a Noonan syndrome-like phenotype and hyperactivated MAPK signaling in humans and mice. J. Clin. Invest. *121*, 3479–3491.
8. Clayton-Smith, J., O'Sullivan, J., Daly, S., Bhaskar, S., Day, R., Anderson, B., Voss, A.K., Thomas, T., Biesecker, L.G., Smith, P., et al. (2011). Whole-exome-sequencing identifies mutations in histone acetyltransferase gene KAT6B in individuals with the Say-Barber-Biesecker variant of Ohdo syndrome. Am. J. Hum. Genet. *89*, 675–681.
9. Simpson, M.A., Deshpande, C., Dafou, D., Vissers, L.E., Woollard, W.J., Holder, S.E., Gillessen-Kaesbach, G., Derks, R., White, S.M., Cohen-Snuijf, R., et al. (2012). De novo mutations of the gene encoding the histone acetyltransferase KAT6B cause Genitopatellar syndrome. Am. J. Hum. Genet. *90*, 290–294.

10. Campeau, P.M., Kim, J.C., Lu, J.T., Schwartzentruber, J.A., Abdul-Rahman, O.A., Schlaubitz, S., Murdock, D.M., Jiang, M.M., Lammer, E.J., Enns, G.M., et al. (2012). Mutations in KAT6B, encoding a histone acetyltransferase, cause Genitopatellar syndrome. Am. J. Hum. Genet. *90*, 282–289.
11. Yu, H.C., Geiger, E.A., Medne, L., Zackai, E.H., and Shaikh, T.H. (2014). An individual with blepharophimosis-ptosis-epicanthus inversus syndrome (BPES) and additional features expands the phenotype associated with mutations in KAT6B. Am. J. Med. Genet. A. *164A*, 950–957.
12. Arboleda, V.A., Lee, H., Dorrani, N., Zadeh, N., Willis, M., Macmurdo, C.F., Manning, M.A., Kwan, A., Hudgins, L., Barthelemy, F., et al.; UCLA Clinical Genomics Center (2015). De novo nonsense mutations in KAT6A, a lysine acetyltransferase gene, cause a syndrome including microcephaly and global developmental delay. Am. J. Hum. Genet. *96*, 498–506.
13. Tham, E., Lindstrand, A., Santani, A., Malmgren, H., Nesbitt, A., Dubbs, H.A., Zackai, E.H., Parker, M.J., Millan, F., Rosenbaum, K., et al. (2015). Dominant mutations in KAT6A cause intellectual disability with recognizable syndromic features. Am. J. Hum. Genet. *96*, 507–513.
14. Vega, H., Waisfisz, Q., Gordillo, M., Sakai, N., Yanagihara, I., Yamada, M., van Gosliga, D., Kayserili, H., Xu, C., Ozono, K., et al. (2005). Roberts syndrome is caused by mutations in ESCO2, a human homolog of yeast ECO1 that is essential for the establishment of sister chromatid cohesion. Nat. Genet. *37*, 468–470.
15. Williams, S.R., Aldred, M.A., Der Kaloustian, V.M., Halal, F., Gowans, G., McLeod, D.R., Zondag, S., Toriello, H.V., Magenis, R.E., and Elsea, S.H. (2010). Haploinsufficiency of HDAC4 causes brachydactyly mental retardation syndrome, with brachydactyly type E, developmental delays, and behavioral problems. Am. J. Hum. Genet. *87*, 219–228.
16. Deardorff, M.A., Bando, M., Nakato, R., Watrin, E., Itoh, T., Minamino, M., Saitoh, K., Komata, M., Katou, Y., Clark, D., et al. (2012). HDAC8 mutations in Cornelia de Lange syndrome affect the cohesin acetylation cycle. Nature *489*, 313–317.
17. Taverna, S.D., Li, H., Ruthenburg, A.J., Allis, C.D., and Patel, D.J. (2007). How chromatin-binding modules interpret histone modifications: lessons from professional pocket pickers. Nat. Struct. Mol. Biol. *14*, 1025–1040.
18. Musselman, C.A., Lalonde, M.E., Côté, J., and Kutateladze, T.G. (2012). Perceiving the epigenetic landscape through histone readers. Nat. Struct. Mol. Biol. *19*, 1218–1227.
19. Doyon, Y., Cayrou, C., Ullah, M., Landry, A.J., Côté, V., Selleck, W., Lane, W.S., Tan, S., Yang, X.J., and Côté, J. (2006). ING tumor suppressor proteins are critical regulators of chromatin acetylation required for genome expression and perpetuation. Mol. Cell *21*, 51–64.
20. Ullah, M., Pelletier, N., Xiao, L., Zhao, S.P., Wang, K., Degerny, C., Tahmasebi, S., Cayrou, C., Doyon, Y., Goh, S.L., et al. (2008). Molecular architecture of quartet MOZ/MORF histone acetyltransferase complexes. Mol. Cell. Biol. *28*, 6828–6843.
21. Lalonde, M.E., Avvakumov, N., Glass, K.C., Joncas, F.H., Saksouk, N., Holliday, M., Paquet, E., Yan, K., Tong, Q., Klein, B.J., et al. (2013). Exchange of associated factors directs a switch in HBO1 acetyltransferase histone tail specificity. Genes Dev. *27*, 2009–2024.
22. Liu, L., Qin, S., Zhang, J., Ji, P., Shi, Y., and Wu, J. (2012). Solution structure of an atypical PHD finger in BRPF2 and its interaction with DNA. J. Struct. Biol. *180*, 165–173.
23. Klein, B.J., Muthurajan, U.M., Lalonde, M.E., Gibson, M.D., Andrews, F.H., Hepler, M., Machida, S., Yan, K., Kurumizaka, H., Poirier, M.G., et al. (2016). Bivalent interaction of the PZP domain of BRPF1 with the nucleosome impacts chromatin dynamics and acetylation. Nucleic Acids Res. *44*, 472–484.
24. Laue, K., Daujat, S., Crump, J.G., Plaster, N., Roehl, H.H., Kimmel, C.B., Schneider, R., Hammerschmidt, M.; and Tübingen 2000 Screen Consortium (2008). The multidomain protein Brpf1 binds histones and is required for Hox gene expression and segmental identity. Development *135*, 1935–1946.
25. You, L., Chen, L., Penney, J., Miao, D., and Yang, X.J. (2014). Expression atlas of the multivalent epigenetic regulator Brpf1 and its requirement for survival of mouse embryos. Epigenetics *9*, 860–872.
26. You, L., Yan, K., Zou, J., Zhao, H., Bertos, N.R., Park, M., Wang, E., and Yang, X.J. (2015). The lysine acetyltransferase activator Brpf1 governs dentate gyrus development through neural stem cells and progenitors. PLoS Genet. *11*, e1005034.
27. You, L., Yan, K., Zou, J., Zhao, H., Bertos, N.R., Park, M., Wang, E., and Yang, X.J. (2015). The chromatin regulator Brpf1 regulates embryo development and cell proliferation. J. Biol. Chem. *290*, 11349–11364.
28. You, L., Zou, J., Zhao, H., Bertos, N.R., Park, M., Wang, E., and Yang, X.J. (2015). Deficiency of the chromatin regulator BRPF1 causes abnormal brain development. J. Biol. Chem. *290*, 7114–7129.
29. You, L., Li, L., Zou, J., Yan, K., Belle, J., Nijnik, A., Wang, E., and Yang, X.J. (2016). BRPF1 is essential for development of fetal hematopoietic stem cells. J. Clin. Invest. *126*, 3247–3262.
30. Ling, P.D., and Huls, H.M. (2005). Isolation and immortalization of lymphocytes. Curr. Protoc. Mol. Biol. *Chapter 28*, unit 28.2.
31. Yan, K., You, L., Degerny, C., Ghorbani, M., Liu, X., Chen, L., Li, L., Miao, D., and Yang, X.J. (2016). The chromatin regulator BRPF3 preferentially activates the HBO1 acetyltransferase but is dispensable for mouse development and survival. J. Biol. Chem. *291*, 2647–2663.
32. Sobreira, N., Schiettecatte, F., Valle, D., and Hamosh, A. (2015). GeneMatcher: a matching tool for connecting investigators with an interest in the same gene. Hum. Mutat. *36*, 928–930.
33. Firth, H.V., Richards, S.M., Bevan, A.P., Clayton, S., Corpas, M., Rajan, D., Van Vooren, S., Moreau, Y., Pettett, R.M., and Carter, N.P. (2009). DECIPHER: Database of Chromosomal Imbalance and Phenotype in Humans Using Ensembl Resources. Am. J. Hum. Genet. *84*, 524–533.
34. Qin, S., Jin, L., Zhang, J., Liu, L., Ji, P., Wu, M., Wu, J., and Shi, Y. (2011). Recognition of unmodified histone H3 by the first PHD finger of bromodomain-PHD finger protein 2 provides insights into the regulation of histone acetyltransferases monocytic leukemic zinc-finger protein (MOZ) and MOZ-related factor (MORF). J. Biol. Chem. *286*, 36944–36955.
35. Poplawski, A., Hu, K., Lee, W., Natesan, S., Peng, D., Carlson, S., Shi, X., Balaz, S., Markley, J.L., and Glass, K.C. (2014). Molecular insights into the recognition of N-terminal histone modifications by the BRPF1 bromodomain. J. Mol. Biol. *426*, 1661–1676.
36. Vezzoli, A., Bonadies, N., Allen, M.D., Freund, S.M., Santiveri, C.M., Kvinlaug, B.T., Huntly, B.J., Göttgens, B., and Bycroft, M. (2010). Molecular basis of histone H3K36me3 recognition

by the PWWP domain of Brpf1. Nat. Struct. Mol. Biol. *17*, 617–619.
37. Wu, H., Zeng, H., Lam, R., Tempel, W., Amaya, M.F., Xu, C., Dombrovski, L., Qiu, W., Wang, Y., and Min, J. (2011). Structural and histone binding ability characterizations of human PWWP domains. PLoS ONE *6*, e18919.
38. Huang, F., Paulson, A., Dutta, A., Venkatesh, S., Smolle, M., Abmayr, S.M., and Workman, J.L. (2014). Histone acetyltransferase Enok regulates oocyte polarization by promoting expression of the actin nucleation factor spire. Genes Dev. *28*, 2750–2763.
39. Huang, F., Saraf, A., Florens, L., Kusch, T., Swanson, S.K., Szerszen, L.T., Li, G., Dutta, A., Washburn, M.P., Abmayr, S.M., and Workman, J.L. (2016). The Enok acetyltransferase complex interacts with Elg1 and negatively regulates PCNA unloading to promote the G1/S transition. Genes Dev. *30*, 1198–1210.
40. Feng, Y., Vlassis, A., Roques, C., Lalonde, M.E., González-Aguilera, C., Lambert, J.P., Lee, S.B., Zhao, X., Alabert, C., Johansen, J.V., et al. (2016). BRPF3-HBO1 regulates replication origin activation and histone H3K14 acetylation. EMBO J. *35*, 176–192.
41. Thomas, T., Voss, A.K., Chowdhury, K., and Gruss, P. (2000). Querkopf, a MYST family histone acetyltransferase, is required for normal cerebral cortex development. Development *127*, 2537–2548.
42. Strübbe, G., Popp, C., Schmidt, A., Pauli, A., Ringrose, L., Beisel, C., and Paro, R. (2011). Polycomb purification by in vivo biotinylation tagging reveals cohesin and Trithorax group proteins as interaction partners. Proc. Natl. Acad. Sci. USA *108*, 5572–5577.
43. Champagne, N., Bertos, N.R., Pelletier, N., Wang, A.H., Vezmar, M., Yang, Y., Heng, H.H., and Yang, X.J. (1999). Identification of a human histone acetyltransferase related to monocytic leukemia zinc finger protein. J. Biol. Chem. *274*, 28528–28536.
44. Simó-Riudalbas, L., Pérez-Salvia, M., Setien, F., Villanueva, A., Moutinho, C., Martínez-Cardús, A., Moran, S., Berdasco, M., Gomez, A., Vidal, E., et al. (2015). KAT6B Is a Tumor Suppressor Histone H3 Lysine 23 Acetyltransferase Undergoing Genomic Loss in Small Cell Lung Cancer. Cancer Res. *75*, 3936–3945.
45. Vandamme, J., Sidoli, S., Mariani, L., Friis, C., Christensen, J., Helin, K., Jensen, O.N., and Salcini, A.E. (2015). H3K23me2 is a new heterochromatic mark in Caenorhabditis elegans. Nucleic Acids Res. *43*, 9694–9710.
46. Chen, S., Yang, Z., Wilkinson, A.W., Deshpande, A.J., Sidoli, S., Krajewski, K., Strahl, B.D., Garcia, B.A., Armstrong, S.A., Patel, D.J., and Gozani, O. (2015). The PZP Domain of AF10 Senses Unmodified H3K27 to Regulate DOT1L-Mediated Methylation of H3K79. Mol. Cell *60*, 319–327.
47. Zhou, T., Chung, Y.H., Chen, J., and Chen, Y. (2016). Site-Specific Identification of Lysine Acetylation Stoichiometries in Mammalian Cells. J. Proteome Res. *15*, 1103–1113.
48. Tsai, W.W., Wang, Z., Yiu, T.T., Akdemir, K.C., Xia, W., Winter, S., Tsai, C.Y., Shi, X., Schwarzer, D., Plunkett, W., et al. (2010). TRIM24 links a non-canonical histone signature to breast cancer. Nature *468*, 927–932.
49. Nishiyama, A., Yamaguchi, L., Sharif, J., Johmura, Y., Kawamura, T., Nakanishi, K., Shimamura, S., Arita, K., Kodama, T., Ishikawa, F., et al. (2013). Uhrf1-dependent H3K23 ubiquitylation couples maintenance DNA methylation and replication. Nature *502*, 249–253.
50. Papazyan, R., Voronina, E., Chapman, J.R., Luperchio, T.R., Gilbert, T.M., Meier, E., Mackintosh, S.G., Shabanowitz, J., Tackett, A.J., Reddy, K.L., et al. (2014). Methylation of histone H3K23 blocks DNA damage in pericentric heterochromatin during meiosis. eLife *3*, e02996.
51. Yang, X.J. (2015). MOZ and MORF acetyltransferases: Molecular interaction, animal development and human disease. Biochim. Biophys. Acta *1853*, 1818–1826.
52. O'Meara, M.M., Zhang, F., and Hobert, O. (2010). Maintenance of neuronal laterality in Caenorhabditis elegans through MYST histone acetyltransferase complex components LSY-12, LSY-13 and LIN-49. Genetics *186*, 1497–1502.
53. Scott, E.K., Lee, T., and Luo, L. (2001). enok encodes a Drosophila putative histone acetyltransferase required for mushroom body neuroblast proliferation. Curr. Biol. *11*, 99–104.
54. Berger, J., Senti, K.A., Senti, G., Newsome, T.P., Asling, B., Dickson, B.J., and Suzuki, T. (2008). Systematic identification of genes that regulate neuronal wiring in the Drosophila visual system. PLoS Genet. *4*, e1000085.
55. Miller, C.T., Maves, L., and Kimmel, C.B. (2004). moz regulates Hox expression and pharyngeal segmental identity in zebrafish. Development *131*, 2443–2461.
56. Katsumoto, T., Aikawa, Y., Iwama, A., Ueda, S., Ichikawa, H., Ochiya, T., and Kitabayashi, I. (2006). MOZ is essential for maintenance of hematopoietic stem cells. Genes Dev. *20*, 1321–1330.
57. Thomas, T., Corcoran, L.M., Gugasyan, R., Dixon, M.P., Brodnicki, T., Nutt, S.L., Metcalf, D., and Voss, A.K. (2006). Monocytic leukemia zinc finger protein is essential for the development of long-term reconstituting hematopoietic stem cells. Genes Dev. *20*, 1175–1186.

The American Journal of Human Genetics, Volume *100*

Supplemental Data

Mutations in the Chromatin Regulator Gene *BRPF1* Cause Syndromic Intellectual Disability and Deficient Histone Acetylation

Kezhi Yan, Justine Rousseau, Rebecca Okashah Littlejohn, Courtney Kiss, Anna Lehman, Jill A. Rosenfeld, Constance T.R. Stumpel, Alexander P.A. Stegmann, Laurie Robak, Fernando Scaglia, Thi Tuyet Mai Nguyen, He Fu, Norbert F. Ajeawung, Maria Vittoria Camurri, Lin Li, Alice Gardham, Bianca Panis, Mohammed Almannai, Maria J. Guillen Sacoto, Berivan Baskin, Claudia Ruivenkamp, Fan Xia, Weimin Bi, DDD Study, CAUSES Study, Megan T. Cho, Thomas P. Potjer, Gijs W.E. Santen, Michael J. Parker, Natalie Canham, Margaret McKinnon, Lorraine Potocki, Jennifer J. MacKenzie, Elizabeth R. Roeder, Philippe M. Campeau, and Xiang-Jiao Yang

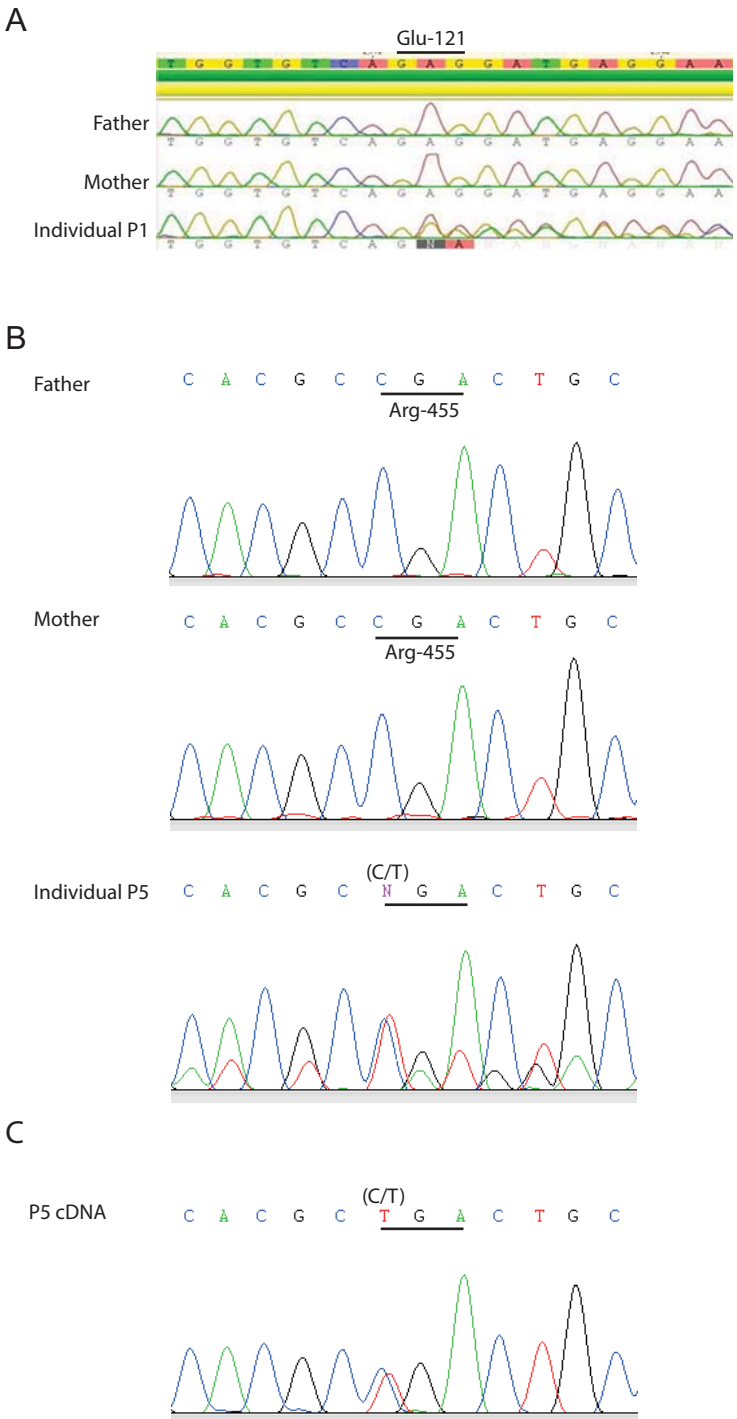

Figure S1. Confirmation of two de novo BRPF1 mutations by Sanger sequencing

(A) Sanger sequencing chromatograms of genomic DNA from individual P1 and her parents. Only the region around the mutation site is displayed here. Unlike her parents, she contains an AG deletion (c.362_363delAG, Table 1), which introduces a reading-frame shift starting at the codon for Glu-121 of BRPF1.

(B) Sequencing chromatograms of genomic DNA from individual P5 and her parents. Only the region at the mutation site is shown here. Unlike her parents, she is heterozygous for the mutation c.1363C>T (Table 1). In the mutated allele, the mutation introduces a TGA stop codon that replaces the codon for Arg-455 of BRPF1.

(C) Sanger sequencing chromatogram of fibroblast cDNA from individual P5. The results not only confirm that she is heterozygous for the mutation c.1363C>T, but also show that the normal and mutant alleles are expressed to similar levels.

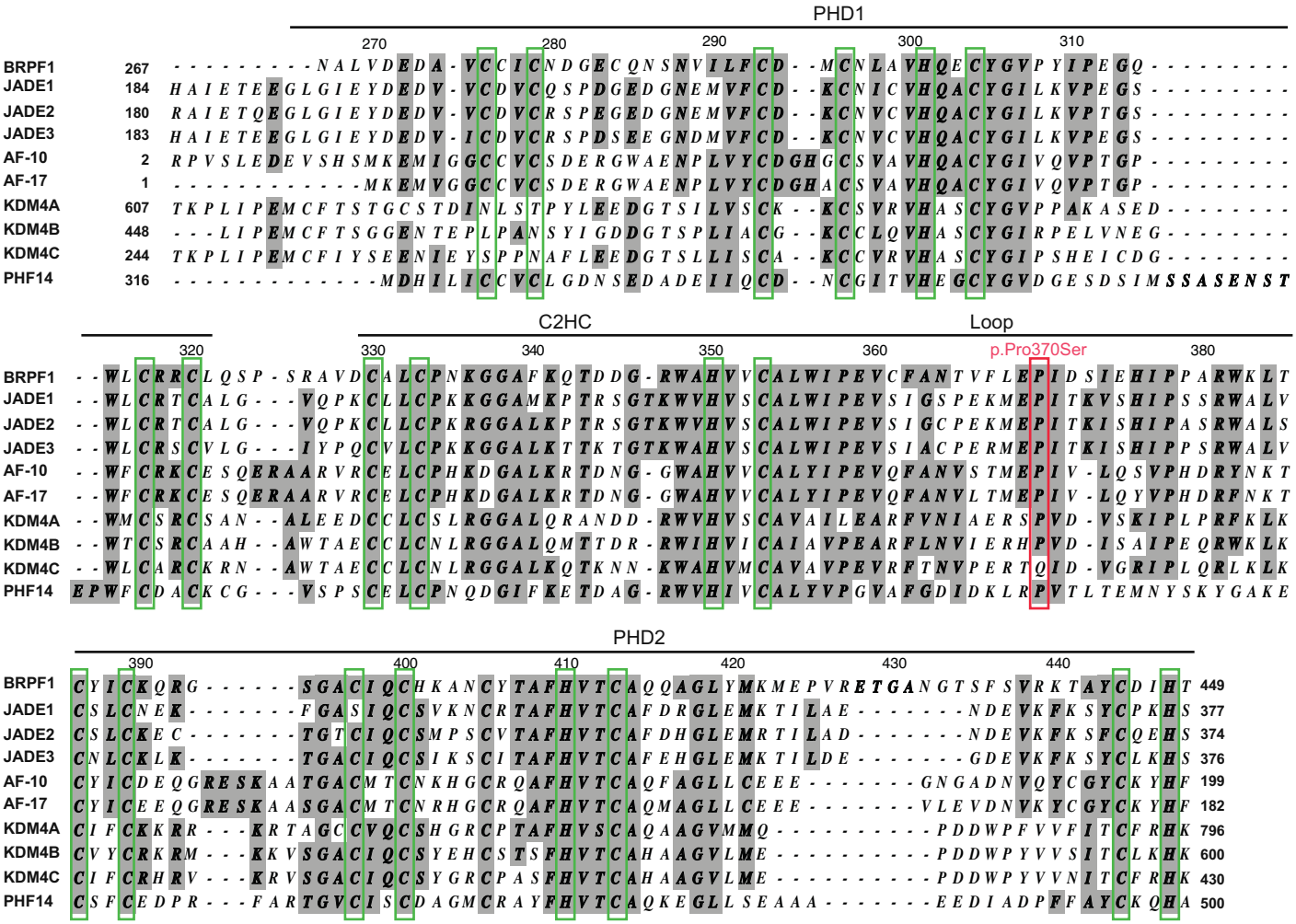

Figure S2. Sequence comparison of PZP domains in BRPF1 and other human proteins

The sequence of human BRPF1 (residues 267-449) was aligned with homologous regions of three JADE proteins (JAED1, JADE2 and JADE3), two leukemia translocation partners (AF-10 and AF-17), three histone demethylases (KDM4A, KDM4B and KDM4C) and PHD finger protein 14 (PHF14). Pro-370 of BRPF1 and its corresponding residues in other PZP proteins are boxed in red. Cysteine and histidine residues involved in zinc chelating to form zinc fingers are boxed in light green. To generate the alignment, the sequence of human BRPF1 (corresponding to residues 267-449) was used as bait for BLAST search against the human protein sequence database at the NCBI BLAST search website. Homologous sequences were then downloaded to MacVector for alignment of residues 267-449 of BRPF1 to other PZP domains. The region corresponding to residues 420-440 was subject to manual editing to align the last two cysteine and histidine residues of different PZP domains. The GenBank accession numbers used are: NP_001003694 (BRPF1), NP_955352 (JADE1), XP_016864771 (JADE2), NP_055550 (JADE3), NP_001182555 (AF-10), NP_005928 (AF-17), XP_005271413 (KDM4A), XP_011526118 (KDMT4B), XP_016869994 (KDM4C) and XP_016868304 (PHF14). Not shown here is the histone methyl-transferase KMT3B (formerly known as NSD1), which also contains a PZP domain but is less conserved.[1]

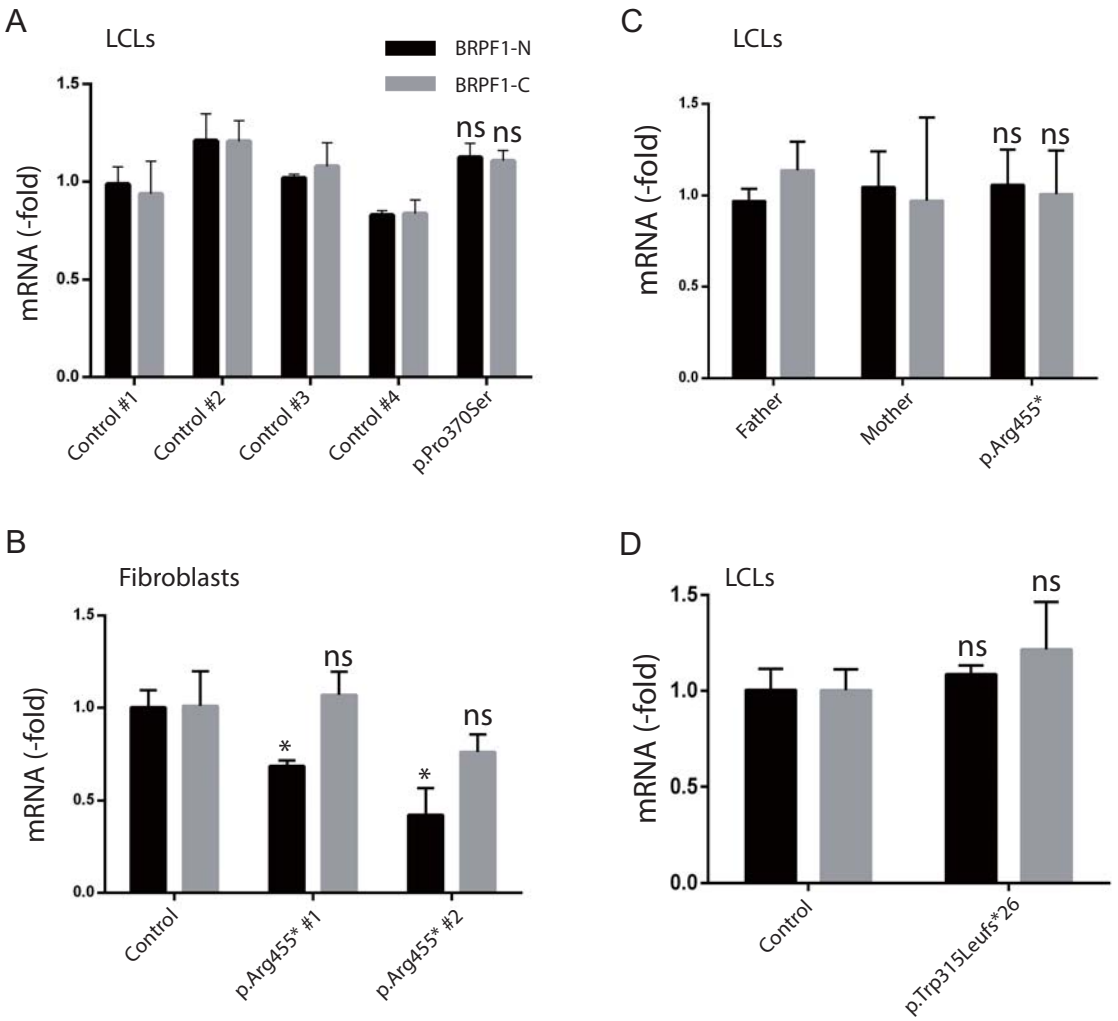

Figure S3. *BRPF1* mRNA levels in normal and mutant cells

(A) RT-qPCR analysis of *BRPF1* mRNA in control and p.Pro370Ser lymphoblastoid cell lines (LCLs). BRPF1-N, RT-qPCR using primers amplifying a region encoding an N-terminal part of BRPF1; BRPF1-C, RT-qPCR using primers amplifying a region encoding a C-terminal part of BRPF1.

(B) Analysis of *BRPF1* mRNA in control and p.Arg455* fibroblasts. Two different batches of fibroblasts were tested. RT-qPCR primers were the same as those used in (A).

(C) RT-qPCR analysis of *BRPF1* mRNA in LCLs prepared from individual P5 (encoding the variant p.Arg455*) and her parents.

(D) Analysis of *BRPF1* mRNA in control and p.Trp315Leufs*26 LCLs. RT-qPCR primers were the same as those used in (A). The experiments in (A-D) were repeated three times and mean values are presented with standard deviations. ns, not statistically significant when compared to the corresponding control(s); *, $p<0.05$.

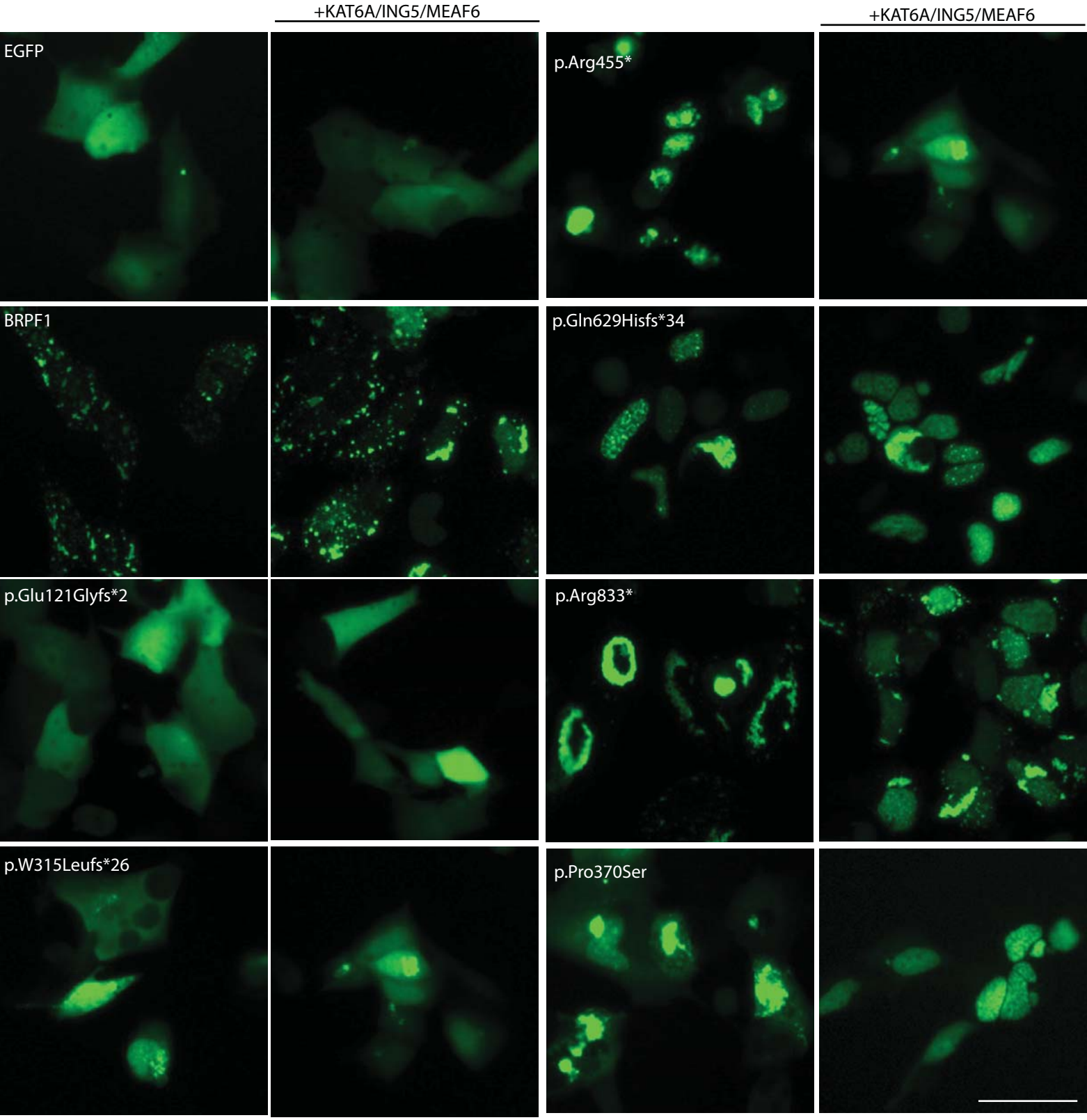

Figure S4. Subcellular localization of BRPF1 and its variants

BRPF1 and its variants were produced as EGFP-tagged fusion proteins in HEK293 cells, with or without exogeneous KAT6A, ING5 and MEAF6 as indicated. EGFP itself was used as the negative control. About 18 h post-transfection, GFP signals were determined by live fluorescence microscopy. For NIH3T3 fibroblasts, it is known that BRPF1 formed cytoplasmic dots but became nuclear when KAT6A was also produced.[2] Images shown here were taken 18 h after transfection. In the presence of exogeneous KAT6A, ING5 and MEAF6, BRPF1 was mainly cytoplasmic at that time (as shown here), but became mainly nuclear in 50% cells at 36 h after transfection (data not shown). No such changes were found when BRPF1 was produced alone (data not shown). Scale bar, 50 μm.

Table S1. Detailed features of 10 individuals with heterozygous *BRPF1* mutations

Individuals	P1	P2	P3	P4	P5	P6	P7	P8	P9	P10
Gender	Female	Male	Female	Male	Female	Male	Male	Female	Female	Female
Mutation in NM_001003694.1	c.362_363 delAG	c.942_955 del	c.942_955 del	c.1108C>T	c.1363C>T	c.1688_ 1689del	c.1883_ 1886dup	c.2497C>T	c.2915dup C	c.3298C>T
Alteration in BRPF1	p.Glu121Gly fs*2	p.Trp315Leu fs*26	p.Trp315Leu fs*26	p.Pro370Ser	p.Arg455*	p.His563 Profs*8	p.Gln629 Hisfs*34	p.Arg833*	p.Met973 Asnfs*24	p.Arg1100*
Mode of transmission	*De novo*	Parental samples not available	Parental samples not available	Mosaic in unaffected mother (mosaicism, 7% in blood DNA, based exome sequencing reads)	*De novo*	*De novo*	*De novo*	*De novo*	*De novo*	*De novo*
Family history	2 older healthy maternal half-siblings. Mother with history of meningioma. Father with joint hypermobility. No consanguinity.	Similarly affected full sibling (P3). Biological mother with intellectual disability.	Similarly affected full sibling (P2). Biological mother with intellectual disability.	2 sisters in good health. Brother has dyslexia and learning difficulties. No history of birth defects, learning difficulties, mental retardation or inherited disorders. No consanguinity.	Nil significant	One brother IQ 120, normal development, ADHD. Parents both ADHD but with university degrees.	Nil significant	Paternal uncle has Tourette	Nil significant	Healthy younger sister
Pregnancy issues	Polyhydramnios, subjective	Uncertain prenatal history.	Uncertain prenatal history.	No	Maternal diabetes	No	Early twin loss	None	1st trimester bleed, nil	Ultrasound at 20 weeks soft-

	decreased fetal movements								else	marker at heart
Delivery issues (specify gestational age)	42 weeks, SROM, SVD	38 weeks. Tracheomalacia, Placed in foster care within first week of life as mother with ID. Father with cerebral palsy. An older sister had been adopted out.	Uncertain, though no known birth complications. Adopted at age of 17 months.	No, delivered at 39 weeks gestation	37w, SVD forceps, apgar 4-8, features consistent with Erb's palsy noted	Born at term Amniotic liquor, needed some extra oxygen Discharged from hospital within hours	Post-term; induced; NVD	40/40	37/40	34 5/7 weeks
Birth weight	7lb 13oz	7lb 12oz	NA	8 lb 3 oz	3955 g	3500 g	3.54 kg	2.7 kg	5lb 70z	2145 g
Birth length	NA	uncertain	NA	21 inches	NA	49 cm	NA	NA	NA	44 cm
Birth head circumference	NA	50th percentile	NA	NA	NA	NA	NA	NA	NA	32.6 cm
Neonatal issues	No major concerns	Tracheomalacia, hypothyroid. GERD, mild RAD, FTT	NA	Failure to thrive but resolved (had esophageal ulcer, peptic esophagitis and patulous gastroesophageal junction)	Neonatal hypertrophic cardiomyopathy, resolved	Little sleep, did not ask for feeding but no real feeding difficulties	Poor feeding	None	none	Hypotonia and tube feeding necessary
Gross motor delay	Hypotonia, delay (sat 12 months; walked at 27 months)	Crawled 14m; walked 16months; GDD now ID. Toe walked	Not recognized or reported	Hypotonia	Yes	Did not turn around or crawl, needed physiotherapy, could crawl at 15 months	First walked ~2 years old	None	Walked at the age of 3, never more than short distances achieved	Hypotonia, yes, walked when 2.5 years old

						and walk (unsteady) at 18 months				
Fine motor delay	mild	Yes	Yes, problems with significant bilateral fine motor coordination	NA	Yes	Normal	NA	Delayed	Palmar grip only	NI
Language delay	Yes, Expressive> receptive	Yes	Yes	Yes and speech apraxia	Yes	Delayed, spoke few words, language understanding and production was delayed. Has a low vocabulary	Speech delay	Moderate	2 single words, 1st at 3	yes
Developmental delay or intellectual disability (please specify severity)	Global developmental delay; discrepant results on cognitive assessment: overall IQ 23rd % ile (WPPSI-III) but low skills in general language index (9th %ile), and extremely low in visual	Yes: GDD noted during infancy. At 7y10m: significant developmental problems in the area of language, visual perceptual fine motor problem solving and gross motor areas. He continues to	At 11 years old, intellectual functioning was assessed with the WISC-IV and found to be in the low average range with a Full Scale IQ of 88. Evaluation by psychiatry at the age of	global development delay (more prominent in expressive language), intellectual functioning disability	DD and ID	IQ 80-100 (brother and parents ≥120) Severe autism, Gilles de la Tourette, ADHD	Mild (main-stream school with extra help)	Mild-moderate ID	Severe ID	Mild ID IQ 56

	perception skills (1st %ile)	have his weakest area in the gross motor area. General developmental age is around 3 to 3-1/2 years of age.	14 years. documents more concerning history: defiant, oppositional, odd, episodes of encopresis at school. No autism. Functions lower than cognitive testing.							
Seizures	no	Yes; diagnosed with epilepsy with generalized tonic clonic seizures infrequently, now seizure free x2 years. Has been off AEDs for several months.	Yes, localization related epilepsy (partial seizures with secondary generalization, diagnosed at age 8y. Rx with AEDs x4years. Now off meds and. Seizure free	No. EEG abnormal (treated with Trileptal and 30lb weight gain, but no clinical seizures).	Episodes of staring spells, consistent with absence seizures. However, EEG only showed high-voltage hypnagogic hypersynchrony, without epileptiform activity.	No	Yes (from 5/52)	None	Multiple types, not controlled by medication, evolving	No
Other neurological abnormalities	Hypotonia, decreased muscle bulk with hyperextensible joints	Mild optic nerve hypoplasia. Mild Central sleep apnea.	Optic nerve slightly small.	NA	ADHD, dyspraxia, social processing disorder. hypotonia	Hypotonic in infancy	Sleep disturbance (melatonin)	Diagnosed with autistic spectrum disorder age 12	Progressive leg contractures secondary to muscular tightening	

Brain MRI	(June 2012): Hyper-intensities of the cortical white matter of the frontal lobes bilaterally.	Paucity of WM, thinning of corpus callosum. Small focus of gliotic change, possibly secondary to remote insult, in the anterior portion of right centrum semi-ovale.	Normal	Normal	Normal	Not done	NA	Not done	Global lack of white matter bulk only	At ultrasound 2 small supependymal cysts. MRI in conclusion after revision normal
Age at last follow-up	6.5 y	13y 3m	13y 10m	11y 2m	8	13	15 y	8 y	17 y	12 y
Weight at last follow-up	33kg (97th % ile)	37.4kg (10th; Z=-1.28)	Weight 73rd percentile	49.5kg (91st %), general appearance overweight	48.1k	45,4 kg (+0,2 SDS)	33.5kg/75-91 [aged 9 on 23.8.06]	32.6kg	43.5kg	57 kg
Height at last follow-up	126 cm (85-97th % ile)	144cm (4th % ; Z=-1.81)	Height 21st percentile	146 cm (58th %)	131.5cm	159 cm (-0,3 SDS)	137.7/50-75 [aged 9 on 23.8.06]	136.3cm	155cm	152 cm
Head circumference at last follow-up	53.5 cm (+1 to +2 SD)	54.5cm (54th %; Z=0.11)	FOC 83rd percentile	52.3 cm	51cm	56 cm (+0,5 SDS) Measured at age 13 yrs 7 months	54.0/25-50 [aged 9 on 23.8.06]	54cm	49cm at age 12	normal
Cranial shape	Normal	Normal	Normal	Mild dolicho-cephaly	Narrow bifrontal diameter	Normal	Normal	Normal	Shape normal but markedly micro-cephalic	normal
Forehead	Narrowing of forehead towards the apex	Normal	Broad, large/tall (Without frank bossing)	Frontal bossing	Normal	broad	Normal	Broad	Normal	Broad
Face, general	Round face, fontal	See below	See below	See below	See below	Sparse facial	See below	Round, dysmorphi	Mildly dysmorphi	Dysmorphic features

	upsweep of hairline,					expressions		c, small chin	c	
Hair	Normal	Upsweep of furontal hair line; normal texture and distribution	Upsweep of frontal hair line. Normal texture and distribution.	Texture: mild hair on upper lip area. Pattern and color: central and hair whorls, some tapering of the posterior hairline laterally along the neck but hairline is not low overall.	Normal	cowlick	Normal	High frontal hairline	Low frontal hairline	normal
Eye dysmorphisms	Right-sided ptosis, hooded eyelids, upslanting palpebral fissures, broad and sparse lateral eyebrows	Hyperteloric. IPD: 6.2 (~97%ile); IC: 3.5/ OC: 9.5/ PF: 3.0) Mild down-slant of PFs Full and robust eyebrows	Appears to have ptosis	Narrow palpebral fissures Synophrys. Straight eyebrows. Narrow palpebral fissures seen in earlier age.	Blepharop himosis, ptosis, medial flaring of eyebrows, hypertelori sm, upslanting palpebral fissures	Ptosis	Down-slanting palpebral fissures	Hypertelori c	Normal	Epicanthal folds, short palpebral fissures, hypertelori sm
Vision	Farsighted	Hyperopia since early childhood// in addition has become more myopic with age	At age 13: Nystagmus, likely congenital. good vision with both eyes open Optic nerves are slightly small in size. Compound hyperopic astigmatism,	Normal	Normal	60%, amblyopi a, +4 dpt glasses. No inner eye abnormal ities	Normal	Has a tendency to squint but no visual deficiency identified	Has a tendency to squint but no visual deficiency identified	normal

Ear dysmorphisms	Normal in form with thick, fleshy ear helices.	Ears look small but measure between 25-50 percentile (5.5/5.8cm) Right ear (5.5cm) is minimally low set. (see photo)	Normal	Small right-sided Darwinian tubercule	Simple superior helices	Prominent conchae, small earlobes	Relatively small ears	Simple, low set, posteriorly rotated	Large, mildly low set	Relatively simple formed
Hearing	normal	Normal	Normal	Normal	Normal	Normal	Normal	Normal	Normal	Normal
Nose		Fleshy nose. Small nostrils.	Fleshy nasal tip with small nostrils.	Full nasal ridge. Lateral buildup to the nose. Bulbous tip. Somewhat pointed nasal tip and narrow nares.	Flat nasal root, relatively small	Normal		Normal	Normal	Flat nasal bridge
Mouth	cupid's bow upper lip,	Short philtrum. Small mouth/ (was micrognathic as younger child). Currently with malocclusion /"cross bite". Teeth extracted for crowding. Needed to have primary teeth extracted as they did not fall out when the adult teeth came	Short philtrum. Mouth normal.	Small mouth, upper lip is somewhat thin and overhanging there is a cupids bow, mildly smooth philtral pillars. Micrognathia	Relatively small, downturned corners of the mouth	Normal		Full upper lip, widely spaced teeth	Wide mouth, upturned upper lip, short philtrum, widely spaced teeth	Normal, full lips

		in. Now has orthodontics in place.								
Palate	Widely spaced teeth, prominent upper incisors, high-arched palate,	Narrow. Normal arch. Normal uvula.	Normal	Teeth and gums overjet	Normal	High arched	Bifid uvula	normal	normal	normal
Hands	Hyperextensible joints of the hands: thumbs at MCPs, distal and proximal IP joints except for 5th MCPs. Hand lengths normal (75th %ile). Normal hand creases.	Normal	Normal	Slightly squared thumbs, minimal degree cubitus valgus. Bridged transverse palmar creases bilaterally seen at age 5.	Left digitalized thumb with small extra bone (phalanx?). Bilateral 5th finger clino-dactyly	Normal	Fifth finger clino-dactyly	Short, broad fingertips	Long, tapering fingers	Normal, atypical palmar creases
Feet	Relatively short feet (25th %ile in length) with 5th toe medial clinodactyly, bilateral metatarsus adductus	Normal	Normal	Mild two-three toe syndactyly	Normal	overpronation of ankles	NA	Normal	Normal	normal
Heart	Normal examination	Normal examination	Normal examination	Normal	Small patent ductus arteriosus, biventricular hypertrophic	Normal examination	Normal examination	Normal	Normal	Mild pulmonary stenosis

					cardiomyopathy thought to be secondary to maternal diabetes (resolved), atrial septal defect					
Kidneys	NA	Normal RUS	Normal RUS/MRI Normal VCUG (workup for enuresis)	NA	NA	Not evaluated	NA	NA	Normal	normal
Feeding difficulties	No	FTT as infant with severe GERD. Had G-tube placed (with fundo) (has since been removed). Major feeding/GI issues as a younger child with gastroparesis, dysmotility. Prompted anal manometry (normal).	None known.	Neonatal period	No	Poor oral motor function (burping, munching, making a mess). Normal appetite	Yes	Reflux, nil else	None	Neonatal and as a baby
Other genetic findings (see note 2)	None	Hetero-zygous pathogenic variant of *MPDZ,* but no signs of	Hetero-zygous pathogenic variant of *MPDZ,* but no signs of	*De novo* duplication of ARID1B gene. Inactivating *ARID1B*	BRAF c.956C>T p.Ser319 Phe BRAF mutations in Noonan	No other pathogenic mutatons were found on	None	Compound mutations in *AIPL*, but one is benign. c.805G>A	Possibly pathogenic *de novo* mutation in *CBL* (c.1145A>	*PIK3R1*: NM_18152 c.1290del, p.Lys430 Asnfs*14, hetero-

		severe congenital hydro-cephalus, caused by *MPDZ* mutations.	severe congenital hydro-cephalus, caused by *MPDZ* mutations.	mutations in Coffin-Siris syndrome, but impact of *ARID1B* duplication remains unknown.	syndrome, but this mutation is benign.	exome. SNP-array was normal		(p.Gly269Arg) & c.401A>T (p.Tyr 134Phe). *AIPL* mutations in leber congenital amaurosis (retinal dystrophy)	T p.Lys382Ile.) but no signs of Noonan syndrome. Compound mutations in *TTI2*: c.1274A>C (p.His416 Pro) & c.1100C>T (Pro367Leu), but the first is probably benign. TTI2 forms a trimeric complex with two other proteins, one of which is linked to syndromic ID, but with much more severe clinical features.	zygous, a*nd de novo.* But there are no signs of SHORT syndrome, which is known to be caused by *PIK3R1* mutations.
Other clinical features	C spine fusion (C2/C3); Premature adrenarche without central puberty (age 7y); Constipation;	Hypothyroidism at age 2 months, currently with normal TSH off synthroid. C2/C3 fusion. Congenital anomaly of	C2/C3 fusion. Mild disk bulges at C4-C5 and C5-C6	Bruises easily. Medications: albuterol sulphate, amoxicillin, cefdinir, fluticasone, oxcarbazepine, prednisone. Has a few	Joint hypermobility. Enlarged left S1 pedicle, abnormal contour to C2 and 3 with apparent underlying	Hypermobile in large joints of the lower extremities, Delayed toilet training (encopresis,	None	Extremely hypermobile at elbows. Puberty at 9, menarche at 10	Thelarche from 7, two bleeds only, found to be in ovarian failure, with post-menopausal hormone levels at 17	Idiopathic pediatric discus calcification at T11-T12

		T9 with butterfly vertebra. Muscle biopsy: Mild variation in fiber size, focal fiber grouping, increased subsarcolemmal oxidative activity (NADH and COX), increased mitochondria (some enlarged and abnormally shaped), increased neutral lipid. Normal ETC enzyme activities except for mild decrease in NADH:ferricyanide dehydrogenase.		scattered nevi.	segmentation abnormality.	constipation), Asthma eczema				

Notes:

1) Abbreviations: NA, not available; Nl: Normal; DD: developmental delay; ID: Intellectual disability; ADHD: attention deficit hyperactivity disorder.
2) Besides *BRPF1* variants, some individuals harbor mutations in other genes. For example, individual P4 carries a duplication of *ARID1B*, individual P8 expresses two compound *AIPL* variants, individual P9 possesses mutations in the *CBL* and *TTI2* genes, and individual P10 carries a pathogenic *PIK3R1* mutation (Table S1). Most of such genetic variants do not appear to be responsible for the major clinical features that we observed in the individuals (Table 2 and S1). For example, *PIK3R1* mutations have been linked to SHORT syndrome[3] and this individual's dysmorphisms do not resemble those reported in the literature. Cognition is typically normal for individuals with SHORT syndrome,[3] so the intellectual disability and speech delay in individual P10 are very likely due to the *BRPF1* mutation (Tables 1-2 and S1). One possible exception is

the *TTI2* mutation in individual P10. Alterations of TTI2 itself and a close partner have been linked to syndromic intellectual disability,[4,5] but the resulting clinical features are much more severe than those in individual P10. Thus, an interesting possibility to be investigated is whether combined effects of different mutations in *BRPF1* and another gene may contribute to phenotypic variations among the 10 individuals (Tables 2 and S1).

Supplemental References

1. Perry, J. (2006). The Epc-N domain: a predicted protein-protein interaction domain found in select chromatin associated proteins. BMC Genomics 7, 6.
2. Ullah, M., Pelletier, N., Xiao, L., Zhao, S.P., Wang, K., Degerny, C., Tahmasebi, S., Cayrou, C., Doyon, Y., Goh, S.L., Champagne, N., Cote, J., and Yang, X.J. (2008). Molecular architecture of quartet MOZ/MORF histone acetyltransferase complexes. Mol Cell Biol 28, 6828-6843.
3. Dyment, D.A., Smith, A.C., Alcantara, D., Schwartzentruber, J.A., Basel-Vanagaite, L., Curry, C.J., Temple, I.K., Reardon, W., Mansour, S., Haq, M.R., Gilbert, R., Lehmann, O.J., Vanstone, M.R., Beaulieu, C.L., et al. (2013). Mutations in PIK3R1 cause SHORT syndrome. Am J Hum Genet 93, 158-166.
4. Langouet, M., Saadi, A., Rieunier, G., Moutton, S., Siquier-Pernet, K., Fernet, M., Nitschke, P., Munnich, A., Stern, M.H., Chaouch, M., and Colleaux, L. (2013). Mutation in TTI2 reveals a role for triple T complex in human brain development. Hum Mutat 34, 1472-1476.
5. You, J., Sobreira, N.L., Gable, D.L., Jurgens, J., Grange, D.K., Belnap, N., Siniard, A., Szelinger, S., Schrauwen, I., Richholt, R.F., Vallee, S.E., Dinulos, M.B., Valle, D., Armanios, M., et al. (2016). A Syndromic Intellectual Disability Disorder Caused by Variants in TELO2, a Gene Encoding a Component of the TTT Complex. Am J Hum Genet 98, 909-918.